Grad-seq guides the discovery of ProQ as a major small RNA-binding protein

Alexandre Smirnov[a], Konrad U. Förstner[a,b], Erik Holmqvist[a], Andreas Otto[c], Regina Günster[a], Dörte Becher[c], Richard Reinhardt[d], and Jörg Vogel[a,e,1]

[a]RNA Biology Group, Institute of Molecular Infection Biology, University of Würzburg, D-97080 Wurzburg, Germany; [b]Core Unit Systems Medicine, University of Würzburg, D-97080 Wurzburg, Germany; [c]Institute for Microbiology, University of Greifswald, D-17489 Greifswald, Germany; [d]Max Planck Genome Centre Cologne, Max Planck Institute for Plant Breeding Research, D-50829 Cologne, Germany; and [e]Research Centre for Infectious Diseases (ZINF), University of Würzburg, D-97070 Wurzburg, Germany

Edited by Gisela Storz, NIH, Bethesda, MD, and approved July 29, 2016 (received for review June 20, 2016)

The functional annotation of transcriptomes and identification of noncoding RNA (ncRNA) classes has been greatly facilitated by the advent of next-generation RNA sequencing which, by reading the nucleotide order of transcripts, theoretically allows the rapid profiling of all transcripts in a cell. However, primary sequence per se is a poor predictor of function, as ncRNAs dramatically vary in length and structure and often lack identifiable motifs. Therefore, to visualize an informative RNA landscape of organisms with potentially new RNA biology that are emerging from microbiome and environmental studies requires the use of more functionally relevant criteria. One such criterion is the association of RNAs with functionally important cognate RNA-binding proteins. Here we analyze the full ensemble of cellular RNAs using gradient profiling by sequencing (Grad-seq) in the bacterial pathogen *Salmonella enterica*, partitioning its coding and noncoding transcripts based on their network of RNA–protein interactions. In addition to capturing established RNA classes based on their biochemical profiles, the Grad-seq approach enabled the discovery of an overlooked large collective of structured small RNAs that form stable complexes with the conserved protein ProQ. We show that ProQ is an abundant RNA-binding protein with a wide range of ligands and a global influence on *Salmonella* gene expression. Given its generic ability to chart a functional RNA landscape irrespective of transcript length and sequence diversity, Grad-seq promises to define functional RNA classes and major RNA-binding proteins in both model species and genetically intractable organisms.

small RNA | noncoding RNA | RNA–protein interaction | ProQ | Hfq

The genomes of many studied organisms are pervasively transcribed, and a significant proportion of this RNA output is accounted for by noncoding RNA (ncRNA) (1, 2). This collective term encompasses different types of transcripts such as ribosomal, transfer, and other housekeeping RNAs [e.g., signal recognition particle (SRP) and RNase P RNA components, tmRNA, or CRISPR RNAs], and also many regulatory RNA species. The latter group is particularly vast and heterogeneous, and several new classes, such as siRNAs, micro RNAs (miRNAs), PIWI-interacting RNAs (piRNAs), long noncoding RNAs, and various bacterial regulatory small RNAs (sRNAs), have emerged as important modulators of gene expression (3, 4).

The discovery of new RNA classes has been greatly facilitated by next-generation sequencing, which, by reading transcript sequences, theoretically allows the rapid profiling of all RNA molecules in a cell (5, 6). However, the sequence per se has limited predictive power when used to identify classes of functionally related ncRNAs, as these often lack easily identifiable motifs such as the translation signals of protein-coding transcripts. This has been particularly evident for the bacterial sRNAs, which dramatically vary in length and structure within and among bacteria (4, 7). Therefore, an informative description of the ncRNA landscape in any organism necessitates the use of more direct and functionally relevant criteria.

One powerful diagnostic trait for ncRNA classes is their complex formation with particular RNA-binding proteins (RBPs), which, for example, has been used to define Argonaute-associated miRNAs or piRNAs (8, 9). In bacteria, the largest class of post-transcriptional regulators is represented by the sRNAs that associate with the Hfq protein (10, 11). This RNA chaperone both stabilizes bound sRNAs and helps them regulate their mRNA targets via imperfect base pairing (12–15). Together, Hfq and its associated sRNAs impact the expression >20% of all genes in enteric model bacteria such as *Escherichia coli* and *Salmonella enterica* (16, 17). A second widespread class of bacterial sRNAs interact with proteins of the CsrA/RsmA family via GGA motifs. In *E. coli*, the CsrB/C and McaS sRNAs sequester the translational repressor CsrA, which in turn regulates hundreds of mRNAs (18, 19).

Importantly, even the well-characterized model bacteria *E. coli* and *Salmonella* contain many additional sRNAs that lack the motifs recognized by Hfq and CsrA (20–22), whereas other prokaryotes possess functional ncRNAs but no Hfq homolog (7, 23, 24). This strongly suggests that additional global RBPs and associated classes of sRNAs with roles in posttranscriptional regulation exist, but have escaped identification by conventional genetic and biochemical approaches. Here, we have combined a classic biochemical technique with high-throughput analysis to reveal the complete functional RNA landscape of a bacterial cell. Our global partitioning of cellular transcripts based on their biochemical behavior has resulted in the discovery of a domain of posttranscriptional control by ProQ, a widespread RBP with a

Significance

Understanding the functions of cellular transcripts based on their sequence is challenging, in particular for noncoding RNAs, which tend to lack easily recognizable motifs. A more functionally relevant criterion is the association of RNAs with cognate RNA-binding proteins. Here, we describe the gradient profiling by sequencing (Grad-seq) approach to draft global RNA landscapes through partitioning all cellular transcripts into diverse coding and noncoding groups based on their shared RNA–protein interactions. Grad-seq has enabled us to define a large class of structured small RNAs that commonly associate with the conserved RNA-binding protein ProQ and appears to constitute a new branch of posttranscriptional control in bacteria. The generic nature of the Grad-seq approach will help to rapidly describe functional RNA landscapes in numerous understudied microbes.

Author contributions: A.S. and J.V. designed research; A.S., E.H., A.O., R.G., D.B., and R.R. performed research; A.O. and R.R. contributed new reagents/analytic tools; A.S., K.U.F., E.H., A.O., R.G., D.B., R.R., and J.V. analyzed data; and A.S. and J.V. wrote the paper.

The authors declare no conflict of interest.

This article is a PNAS Direct Submission.

Freely available online through the PNAS open access option.

Data deposition: The data reported in this paper have been deposited in the Gene Expression Omnibus (GEO) database, www.ncbi.nlm.nih.gov/geo (accession no. GSE62988).

[1]To whom correspondence should be addressed. Email: joerg.vogel@uni-wuerzburg.de.

This article contains supporting information online at www.pnas.org/lookup/suppl/doi:10.1073/pnas.1609981113/-/DCSupplemental.

previously unknown large suite of cellular targets, which include many highly structured regulatory sRNAs.

Results and Discussion

Global Partitioning of Cellular RNAs by Grad-Seq. To describe the RNP landscape in the model enteric bacterium *S. enterica* serovar Typhimurium (henceforth *Salmonella*), we applied a high-throughput biochemical profiling approach (Grad-seq) (Fig. 1*A*). Grad-seq relies on the sedimentation of cellular RNAs and proteins in a glycerol gradient, which sorts complexes by size and shape and offers a means to assess their involvement in various macromolecular assemblies (25, 26). Following this biochemical partitioning step, we analyzed the RNA content of each of the 20 gradient fractions by Illumina cDNA sequencing and visualized the sedimentation profiles of 3,969 individual *Salmonella* transcripts (*SI Appendix*, Figs. S1 and S2 and Dataset S1). These profiles readily matched the expected distributions of housekeeping RNAs in glycerol gradients, including the 16S and 23S rRNAs, which cosediment with the 30S and 50S ribosomal subunits, respectively, tmRNA and the SRP and RNase P RNA components (Fig. 1*B*). Transfer RNAs primarily exist in small RNPs (average $s^0_{20,w}$ ~5S). Importantly, the tRNA sedimentation profiles (*SI Appendix*, Fig. S1) correspond to those of their main protein partners, namely aminoacyl-tRNA synthetases, tRNA modification enzymes and elongation factor Tu, based on liquid chromatography-tandem MS (LC-MS/MS) detection of 1,326 proteins in total from the same gradient fractions (*SI Appendix*, Fig. S3 and Dataset S2).

Likewise, 6S RNA associates with RNA polymerase holoenzyme (RNAP) to modulate the activity of the transcription machinery (27). We obtained almost congruent profiles of 6S RNA reads and RNAP-derived peptides (Spearman's $0.62 < r < 0.91$, $P < 0.0034$), which matched in-gradient profiles determined by standard techniques (Fig. 1*C*): both indicated the formation of a ~16S complex, corresponding to a previously reported particle of 500–600 kDa (27).

Regulatory ncRNAs were more heterogeneously distributed. For instance, Hfq-associated sRNAs (11) sedimented broadly in fractions 3–7 (average $s^0_{20,w}$ ~11S, or ~350 kDa) with additional peaks in the 30S or 70S ribosome fractions (*SI Appendix*, Fig. S1). Representatives of other functional RNA classes (attenuators, antisense RNAs, Hfq-independent sRNAs) displayed even more disparate distributions, suggesting that they are associated with several distinct RBPs. As expected, mRNAs abundantly populate both the 30S and 70S ribosome fractions (*SI Appendix*, Fig. S1). The mRNA reads in lower molecular weight fractions likely represent untranslated mRNAs in complex with regulatory proteins or stable decay intermediates. Of note, the profile of the dual-function tmRNA, which rescues stalled ribosomes (28), combined profile features of both coding and noncoding RNAs with pronounced peaks in both low molecular weight and 70S fractions (Fig. 1*B* and *SI Appendix*, Fig. S1*A*).

Topology of a Bacterial RNA Interactome. Applying principal component analysis (PCA) to the 3,969 RNA profiles obtained (Fig. 2 and *SI Appendix*, Dataset S1), we observed that transcripts with similar biochemical behavior cosegregated, based on the first two principal components that correlate with the profile complexity, i.e., the number of individual peaks in a profile (PC1), and the sedimentation coefficient of complexes (PC2). This bacterial "RNA universe" exhibits two major branches: the upper protein-coding branch is dominated by mRNAs whose behavior is determined by ribosomal components, whereas the noncoding branch toward the bottom is enriched in ncRNAs that are associated with a variety of low molecular weight complexes. The ncRNAs found in the upper branch of the map mostly consisted

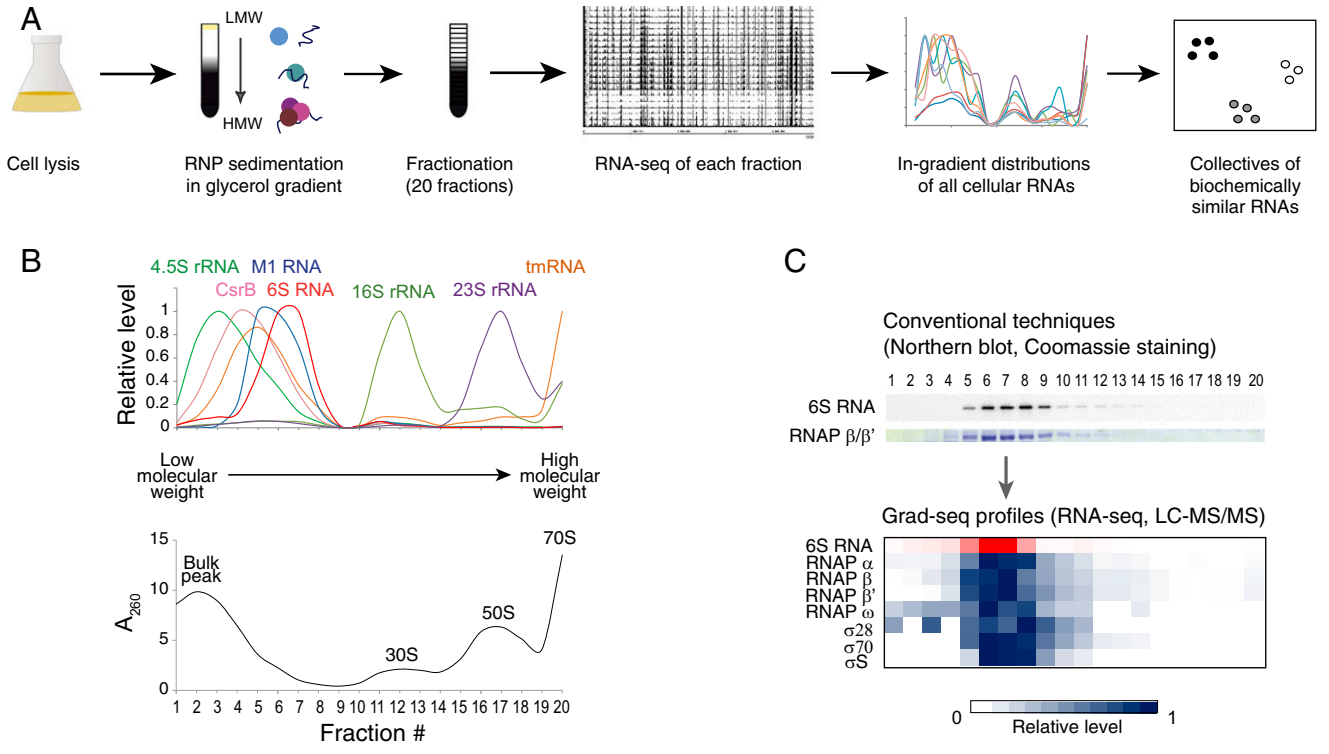

Fig. 1. Grad-seq visualizes the *Salmonella* RNA interactome. (*A*) Grad-seq experimental strategy. (*B*) RNA-seq–based in-gradient distributions of housekeeping RNAs (all profiles are standardized to the range from 0 to 1). M1 and 4.5S RNAs are the RNA subunits of RNase P and SRP, respectively. CsrB is a CsrA-sequestering ncRNA. The UV profile of the corresponding gradient showing the bulk peak of low molecular weight complexes and the positions of ribosomal subunits is provided below. (*C*) The 6S RNA (in complex with the RNA polymerase holoenzyme) visualized with conventional techniques (*Top*, cropped from *SI Appendix*, Fig. S3*A*) and by Grad-seq (heat map below, all profiles are standardized to the range from 0 to 1).

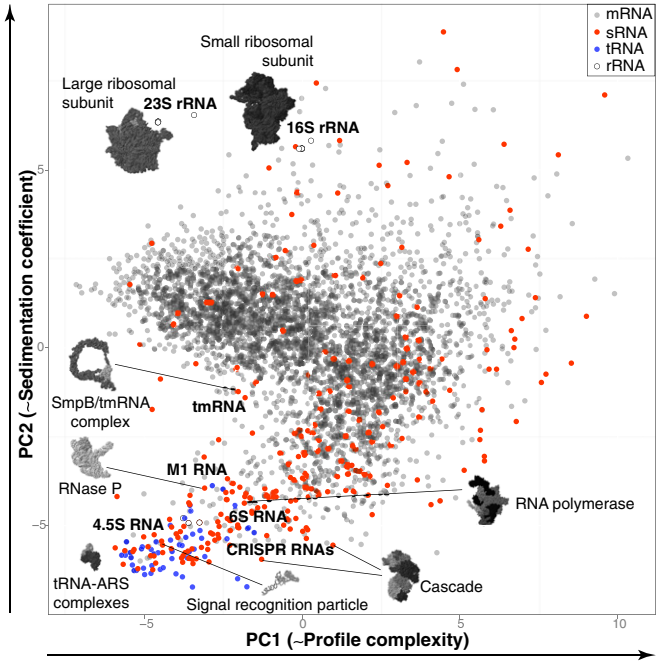

Fig. 2. Topology of the *Salmonella* RNA interactome revealed by PCA of Grad-seq profiles from 3,969 *Salmonella* transcripts. The number of distinct RNPs formed by an RNA increases from *Left* to *Right* (PC1, ~41% of variance), whereas sedimentation coefficients of major RNPs increase from *Bottom* to *Top* (PC2, ~26% of variance). Select examples of corresponding RNPs are provided.

of mRNA-derived sRNAs (overlapping and often processed from UTRs or coding regions of messengers) (16, 29) or misidentified short mRNAs, which explains their association with ribosomal components. Overall, this simple and logical structure reveals the fundamental dichotomy of coding and noncoding RNA functions within the cell, reflected at the level of RNA–protein interactions.

A Cluster of Noncoding RNAs That Interact with Protein ProQ. Focusing the PCA on sRNAs revealed several distinct transcript clusters (Fig. 3*A*). Most well-characterized Hfq-dependent sRNAs (11) form a dense group on this map. Remarkably, even Hfq-associated sRNAs that differ fourfold in length, such as ArcZ (57 nt) and GcvB (206 nt) clustered together (*SI Appendix*, Fig. S4), indicating that biochemical properties rather than sequence determined their in-gradient distributions. Likewise, the CsrA-binding sRNAs (19) CsrB and CsrC (360 and 240 nt, respectively) almost overlapped on the map (Fig. 3*A*). Intriguingly, there are many annotated *Salmonella* sRNAs, including attenuators, *cis*-antisense RNAs and uncharacterized species, that populated the map outside the Hfq- or CsrA-related clusters (Fig. 3*A* and *SI Appendix*, Fig. S4). This raised the possibility that some of these ncRNAs interact with an unknown global RBP.

To identify the associated RBP(s) we tagged 12 sRNAs from outside the Hfq and CsrA clusters with the MS2 aptamer (30) and pulled down interacting proteins from *Salmonella* cell lysates (Fig. 3*A* and *SI Appendix*, Fig. S5). In each case, we detected several candidate protein binding partners. Comparison of sedimentation profiles from our reference proteomics dataset (*SI Appendix*, Fig. S3) with those of the bait sRNAs identified the ProQ protein as the most common and highly correlated partner (Spearman's $0.48 < r < 0.7$, $P < 0.033$, Fig. 3*B*). Western blot analysis confirmed the enrichment of ProQ in sRNA pull-down samples compared with control RNA pull downs (Fig. 3*C*).

ProQ is a FinO-like osmoregulatory protein required for optimal expression of proline channel ProP (31, 32). However, ProQ homologs can be predicted in the chromosomes, plasmids, and bacteriophages of α-, β- and γ-proteobacteria (*SI Appendix*, Fig. S6), many of which lack a *proP* gene. Similarly, the high abundance and constitutive expression of ProQ (33, 34) are also inconsistent with a specialized function: in a semiquantitative Western blot analysis, ProQ levels compare with those of the highly expressed general RBPs, CsrA, Hfq, or ribosomal protein

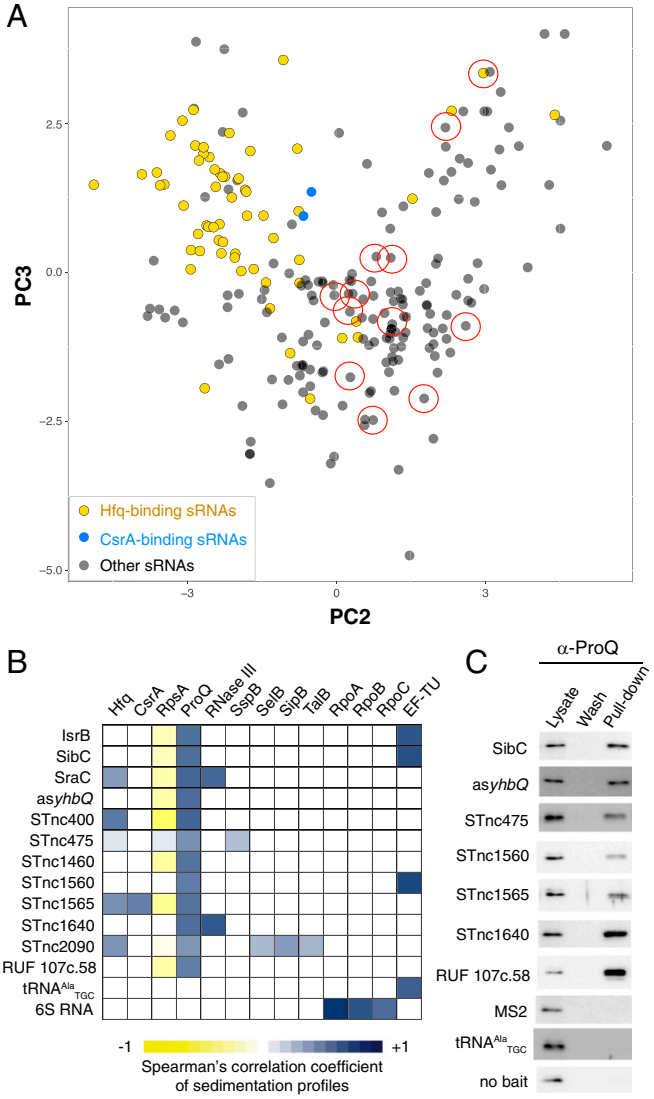

Fig. 3. *Salmonella* sRNA interactome and identification of ProQ as a recurrent sRNA binder. (*A*) Grad-seq PCA plot of 238 *Salmonella* sRNAs. PC2 and PC3 are selected to visualize sRNA clusters with finer detail (*Materials and Methods* provides further information). Only Hfq- and CsrA-associated sRNAs are highlighted (*SI Appendix*, Fig. S4 shows a complete functional sRNA assignment). sRNAs selected for MS2 aptamer tagging and pull down are circled. (*B* and *C*) Pull down of the selected MS2 aptamer-tagged sRNAs from *Salmonella* lysates and identification of their binding partners. (*B*) Heat map showing proteins specifically copurified with each MS2 aptamer-tagged sRNA (most ribosomal proteins are omitted for clarity) and Spearman's correlation coefficients of their sedimentation profiles with the Grad-seq profiles of the bait sRNAs. ProQ is a particularly frequent partner of the selected sRNAs and their sedimentation profiles match, suggesting a stable interaction. (*C*) ProQ is enriched in the MS2 aptamer-tagged sRNA pull downs, compared with control baits or no bait, as visualized with specific antibodies.

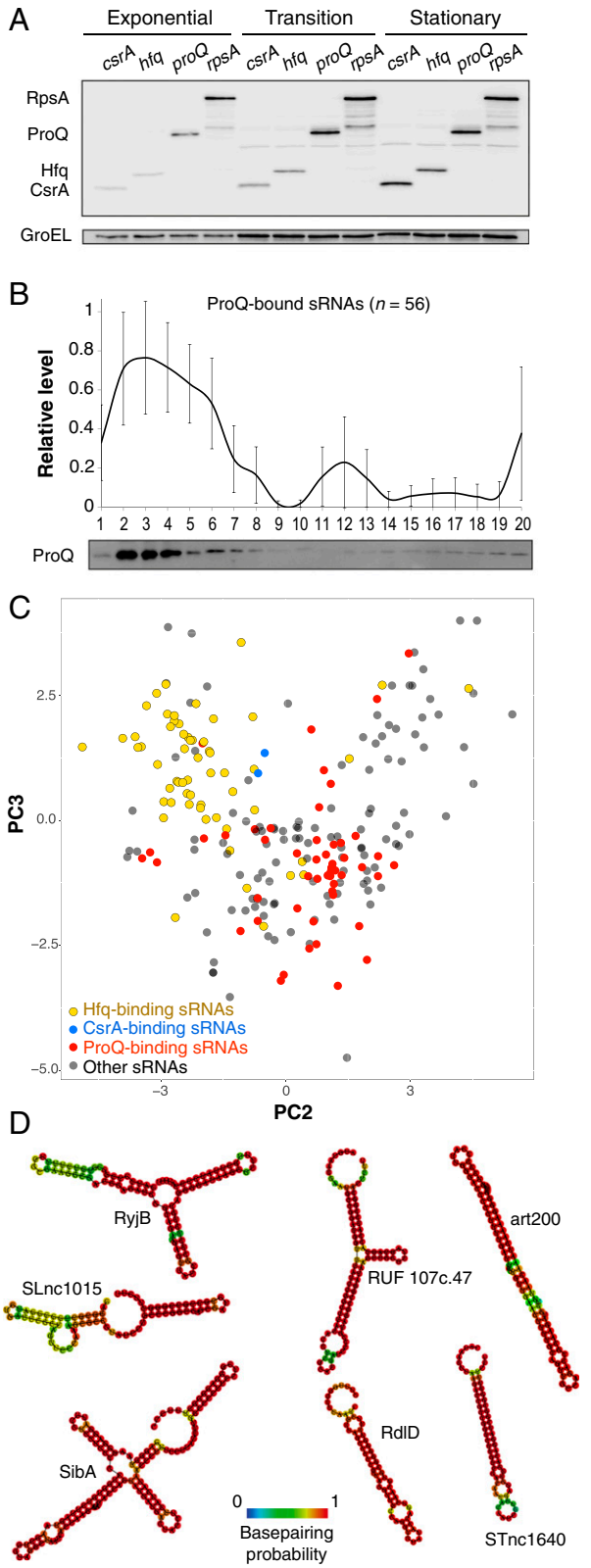

Fig. 4. ProQ is a conserved abundant RNA-binding hub associated with a distinct class of highly structured sRNAs. (*A*) ProQ is an abundant, constitutively expressed protein. Equal amounts of cells with chromosomally FLAG-tagged *csrA*, *hfq*, *proQ*, or *rpsA* genes were analyzed by Western blotting with anti-FLAG antibodies in three growth phases. (*B*) Averaged Grad-seq distribution of ProQ-bound sRNAs. As on *SI Appendix*, Fig. S1*C*, all individual profiles of ProQ-associated sRNAs were cumulated and presented as an average along the gradient ± SD. Corresponding Western blot probed for ProQ is shown below. Only the 56 ProQ-binding sRNAs that are sufficiently covered in the Grad-seq dataset are shown. (*C*) Grad-seq PCA plot of *Salmonella* sRNAs showing segregation of Hfq-, CsrA- and ProQ-binding transcripts (Fig. 3*A* and *SI Appendix*, Fig. S9 *A* and *B* for a complete functional sRNA assignment). (*D*) Minimum free energy secondary structures of representative highly enriched ProQ ligands.

S1 (Fig. 4*A*). Moreover, we find that deletion of *proQ* affects the levels of hundreds of transcripts with no known function in osmoprotection (*SI Appendix*, Fig. S10*A*). Together, these observations suggest a much broader cellular role for ProQ than fine-tuning ProP expression.

ProQ-Associated sRNAs Form a Distinct Group of Riboregulators. To obtain a better understanding of the target suite of ProQ in *Salmonella*, we used RNA immunoprecipitation coupled with deep sequencing. This analysis suggested that ProQ associates with >400 cellular transcripts from diverse cellular pathways (*SI Appendix*, Figs. S7 and S8 and Dataset S3), with small RNAs being significantly overrepresented (98/422, or ∼23.2%, compared with the annotated 547/5,205 or ∼10.5%, $P < 0.0001$, Fisher's exact test). Regarding these noncoding targets (*SI Appendix*, Table S1), ProQ preferentially bound to Hfq-independent sRNAs ($P < 0.0007$, Mann–Whitney test, $P < 0.003$, Kolmogorov–Smirnov test; only two ProQ-bound sRNAs, SraC and STnc520, are known to be Hfq dependent). This suggests the existence of a distinct class of noncoding transcripts, which comprised ∼18% of all currently known *Salmonella* sRNAs, most (>80%) of which are currently uncharacterized. The few ProQ-enriched sRNAs of known function included attenuators (SraF), *trans*-acting base-pairing sRNAs (SraL) (35), sRNA-sequestering sponges (STnc2180) (36), and type I antitoxins (Sib, Rdl, IstR) (24, 37). Diverse types of antisense RNAs (antitoxins, chromosomal, phage and transposon associated), which typically operate in a Hfq-independent manner (24), are particularly overrepresented among ProQ ligands (53/98, or 54%, compared with the annotated 216/547, or ∼39%, $P = 0.008$, Fisher's exact test). As expected, the group of sRNAs used as bait in MS2 aptamer pull-down assays (Fig. 3) showed significantly higher median enrichment in ProQ coimmunoprecipitation compared with all sRNAs ($P < 0.003$, Mann–Whitney test).

ProQ-bound sRNAs formed relatively small RNPs (average $s^0_{20,w}$ ∼7S, corresponding to 100–150 kDa, Fig. 4*B*), and clearly segregated from Hfq- and CsrA-bound transcripts within the sRNA PCA plot (Fig. 4*C* and *SI Appendix*, Fig. S9 *A* and *B*). This separation illustrates the discriminatory power of Grad-seq in identifying collectives of biochemically similar RNAs. EMSAs with purified *Salmonella* ProQ confirmed the high affinity and specific binding of several enriched sRNAs in vitro, supporting their involvement in stable ProQ-containing RNP particles (*SI Appendix*, Fig. S9 *C* and *D*). Top-enriched ProQ sRNA ligands, such as SibA and STnc2090, formed complexes with apparent dissociation constants in the low nanomolar range, similar to the affinities typically observed in interactions of Hfq and CsrA with cognate RNAs (7, 18).

Of note, most ProQ-associated sRNAs form extensively base-paired structures, in some cases resembling eukaryotic miRNA precursors (Fig. 4*D*). A significant positive relationship was observed between the predicted folding energy of *Salmonella* sRNAs and ProQ binding (*SI Appendix*, Fig. S9*E*), suggesting that, similar to the RNA chaperone FinO (32, 38), interactions between ProQ and RNAs are at least partially structure driven. These binding preferences contrast with the typical modes of Hfq (12) or CsrA (39) binding, which use single-stranded regions. Indeed, Hfq-dependent sRNAs, whose only recurrent structured region is the intrinsic terminator stem loop (12), appear to be significantly less folded than ProQ-associated ones (*SI Appendix*, Fig. S9*F*). Thus, ProQ-interacting sRNAs form a structurally distinct class of ncRNAs, and ProQ may fill the niche

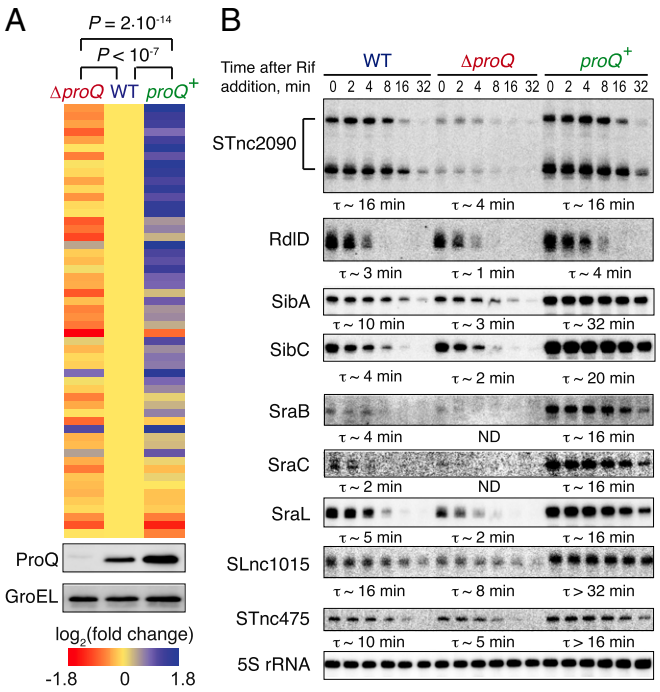

Fig. 5. ProQ acts as a stability factor for most of its sRNA ligands. (*A*) ProQ positively affects the steady-state levels of most of its sRNA ligands. The heat map shows the changes in the abundance of ProQ-associated noncoding RNAs (n = 54) upon *proQ* deletion (Δ*proQ*) or complementation (*proQ*$^+$). Significance of the differences is evaluated by Wilcoxon matched-pairs signed-ranks test. (*Lower*) Corresponding levels of ProQ in these strains, as revealed by Western blotting with a ProQ-specific antiserum. Only those sRNAs that have been sufficiently covered in the transcriptome dataset are shown. (*B*) ProQ stabilizes its associated sRNAs in vivo. Samples from WT, Δ*proQ*, and complemented *proQ*$^+$ strains were collected in the stationary phase after transcription arrest with rifampicin and analyzed by Northern blotting. Approximate half-lives for major detected species are shown below the blots. ND, not determined (<1 min). A representative of three independent experiments is shown.

of a global RBP that associates specifically with highly structured transcripts in bacteria.

Effect of ProQ on Associated RNAs. Association of an RNA with a cellular protein may not necessarily impact its function. However, we found that ProQ affected the abundance of many of its sRNA ligands (Fig. 5), as their cellular levels decreased upon *proQ* deletion (Δ*proQ*); conversely, overexpressing the protein (*proQ*$^+$) increased the levels of most ProQ-associated sRNAs. Furthermore, using the drug rifampicin to arrest bacterial transcription, we observed that in the absence of ProQ the half-lives of several selected ProQ-bound sRNAs were reduced, whereas increased levels of ProQ generally resulted in sRNA overstabilization (Fig. 5*B*). Therefore, ProQ likely protects some of its ligands from degradation and thus may extend the time window for their cellular activity, similar to the FinO protein with its sole known RNA substrate, FinP (40).

As expected from the large suite of ProQ-bound RNAs, *proQ* deletion dramatically affects gene expression in *Salmonella*, changing the levels of >800 transcripts (~16% of genome, *SI Appendix*, Fig. S10*A* and Dataset S4). The pathways significantly overrepresented in the group of differentially regulated genes include energy production, amino acid metabolism, and translation (*SI Appendix*, Fig. S10*B*), indicating that ProQ pervasively impacts bacterial physiology. ProQ seemed to exert both direct and indirect effects on its ligands as ~36% of ProQ-associated RNAs showed significant changes in expression levels (of which ~28% are up-regulated and ~72% are down-regulated upon *proQ* deletion, $P < 0.0001$, Fisher's exact test). Of note, mRNA targets of the few ProQ-dependent sRNAs whose functions are known, such as *cis*-acting Sib antitoxin RNAs (37), were derepressed in response to *proQ* deletion and overrepressed in the *proQ*$^+$ strain (*SI Appendix*, Fig. S10*C* and Dataset S4), suggesting that some of the observed gene expression changes are sRNA mediated. Altogether, these data reveal the existence of a large ProQ-dependent regulon and position ProQ as the third global posttranscriptional gene expression modulator in bacteria besides Hfq and CsrA.

Conclusions

The Grad-seq approach provides an experimental and analytical framework to rapidly visualize the major RNA collectives of an organism of interest, which will be particularly useful in drafting initial functional RNA landscapes for many understudied microbes with unexplored RNA biology (41, 42). With rapidly improving sequencing technologies and decreasing cost, Grad-seq will be able to partition major RNA classes susceptible to therapeutic intervention in medically important microbial communities such as the gut microbiota, the vast majority of whose species remain unculturable.

Grad-seq has conceptual parallels with other methods that have been used to describe the RNP landscape of a cell and efficiently combines their individual strengths. For instance, ribosome profiling (43) employs a similar approach to partition and sequence cellular transcripts but focuses exclusively on those associated with translating ribosomes, whereas Grad-seq also describes smaller RNPs associated with noncoding RNA functions. Similarly, RNPomics (26) aims to enrich and sequence functionally relevant cellular RNA species by separating them from unbound RNA by glycerol gradient centrifugation. However, the resulting RNPs are subsequently studied in bulk, without fractionation, decreasing the resolution of the biochemical information obtained on transcripts. RNA interactome capture (44, 45) is an extremely powerful approach that aims to globally characterize cellular RBPs by deep mass-spectrometric analysis of proteins cross-linked to cellular RNA, but it also operates in bulk, without distinguishing individual RNPs.

A key advantage of Grad-seq is the biochemical grouping of cellular transcripts into RNA collectives of likely similar function, to subsequently identify common protein partners. Although currently a two-step technique, improving the resolution of Grad-seq through finer fractionation, more comprehensive protein detection, and the decreasing costs for RNA-seq may soon permit a more direct approach to match RNA–protein profiles, enabling the analysis of complex eukaryotic systems.

The power of Grad-seq is here illustrated by unveiling ProQ as a global RNA-binding hub in addition to Hfq and CsrA, which is remarkable in light of the extensive previous work on *E. coli* and *Salmonella* as the current workhorses of bacterial RNA research (7). Our discovery of a large class of ProQ-associated sRNAs opens the door for further studies of this potential domain of posttranscriptional control, which will likely reveal molecular mechanisms and physiological roles of RNA in bacteria. Indeed, a recent study in *Legionella* identified a ProQ-like protein as a matchmaker of sRNA–mRNA interactions in the regulation of bacterial competence (46).

Materials and Methods

Bacteria and Media. All bacterial strains and growth conditions are described in *SI Appendix*, Tables S2 and S3.

Grad-Seq. *Salmonella* cells grown to OD_{600} = 2 were lysed in 20 mM Tris·HCl, pH 7.5, 150 mM KCl, 1 mM $MgCl_2$, 1 mM DTT, 1 mM PMSF, 0.2% Triton X-100, 20 units/mL DNase I (Thermo Fisher Scientific), 200 units/mL SUPERase·IN (Life Technologies) with 0.1-mm glass beads (BioSpec Products) on a Retsch MM400 machine. Cleared lysates were centrifuged through linear

10–40% (wt/vol) glycerol gradients in the same buffer formed in Beckman SW40Ti tubes at 100,000 × *g* for 17 h at 4 °C and fractionated in 20 equal fractions. Fractions were deproteinized with 1% SDS and 1 volume of hot phenol by shaking at 55 °C for 5 min, centrifuged, and RNA was precipitated with isopropanol.

For Grad-seq, two biological replicates have been analyzed. Eighty-five picograms per microliter of the spike-in RNA [5′ P-CUCGUCCGACGUCACCUAGA (IBM GmbH)] had been added to each fraction prior to the library preparation. RNA-seq libraries were prepared by Vertis Biotechnologie and sequenced on an Illumina HiSeq 2000 platform. The reads were mapped to the *Salmonella* Typhimurium SL1344 genome with the use of the READemption pipeline version 0.3.4 (47). Fractionwise gene-specific RNA sequencing (RNA-seq) read counts were normalized by corresponding spike-in counts and any remaining uniformly distorting biases were manually removed. All profiles with ≥30 reads in at least one fraction were power transformed to improve linearity and standardized to the range from 0 to 1. To derive averaged distributions for RNA classes, profiles of individual RNAs were summed up and averaged fractionwise. PCA was performed in R and visualized in R and Python. For sRNAs, PC1 mostly reflects the influence of mRNA-derived and overlapping sRNAs (following, like mRNAs, strong ribosomal components) and is uninformative for our purpose of revealing groups of ncRNAs. We opted for PC2 and PC3 analysis instead, which allowed a better resolution and clustering of typical sRNAs. Both PC1 vs. PC2 and PC2 vs. PC3 plots are available on *SI Appendix*, Fig. S4. RNA-seq data are available in Gene Expression Omnibus (accession no. GSE62988). The workflow implemented as Shell script and the analysis-specific tools are deposited at Zenodo at DOI:10.5281/zenodo.35176. All molecular weight estimates provided in this work were made assuming a most frequently encountered moderately elongated shape of particles (25).

Other Methods. Affinity chromatography, RNA coimmunoprecipitation, sRNA turnover, and all statistical analyses are described in detail in *SI Appendix, SI Materials and Methods*.

ACKNOWLEDGMENTS. We thank S. Gorski for editing the manuscript; D. Sheidy, M. Springer, and A. Carpousis for antisera; C. Wang for EMSA and stability samples; R. Rieder, M. Raabe, and S. Grund for the assistance with affinity chromatography and MS; M. Hecker for proteomics infrastructure; T. Achmedov for technical assistance; and members of the J.V. laboratory for comments on the manuscript. The project was supported by funds from the Bavarian BioSysNet Program, the Max Planck Society, and Bundesministerium für Bildung und Forschung Grants Next-Generation Transcriptomics of Bacterial Infections and eBio RNAsys. E.H. is supported by the Wenner-Gren Foundations.

1. Cech TR, Steitz JA (2014) The noncoding RNA revolution-trashing old rules to forge new ones. *Cell* 157(1):77–94.
2. Altman S (2015) Twenty years. *RNA* 21(4):513–514.
3. Patil VS, Zhou R, Rana TM (2014) Gene regulation by non-coding RNAs. *Crit Rev Biochem Mol Biol* 49(1):16–32.
4. Storz G, Vogel J, Wassarman KM (2011) Regulation by small RNAs in bacteria: Expanding frontiers. *Mol Cell* 43(6):880–891.
5. Barquist L, Vogel J (2015) Accelerating discovery and functional analysis of small RNAs with new technologies. *Annu Rev Genet* 49:367–394.
6. Sorek R, Cossart P (2010) Prokaryotic transcriptomics: A new view on regulation, physiology and pathogenicity. *Nat Rev Genet* 11(1):9–16.
7. Wagner EG, Romby P (2015) Small RNAs in bacteria and archaea: Who they are, what they do, and how they do it. *Adv Genet* 90:133–208.
8. Meister G (2013) Argonaute proteins: Functional insights and emerging roles. *Nat Rev Genet* 14(7):447–459.
9. Iwasaki YW, Siomi MC, Siomi H (2015) PIWI-interacting RNA: Its biogenesis and functions. *Annu Rev Biochem* 84:405–433.
10. De Lay N, Schu DJ, Gottesman S (2013) Bacterial small RNA-based negative regulation: Hfq and its accomplices. *J Biol Chem* 288(12):7996–8003.
11. Vogel J, Luisi BF (2011) Hfq and its constellation of RNA. *Nat Rev Microbiol* 9(8):578–589.
12. Ishikawa H, Otaka H, Maki K, Morita T, Aiba H (2012) The functional Hfq-binding module of bacterial sRNAs consists of a double or single hairpin preceded by a U-rich sequence and followed by a 3′ poly(U) tail. *RNA* 18(5):1062–1074.
13. Schu DJ, Zhang A, Gottesman S, Storz G (2015) Alternative Hfq-sRNA interaction modes dictate alternative mRNA recognition. *EMBO J* 34(20):2557–2573.
14. Updegrove TB, Shabalina SA, Storz G (2015) How do base-pairing small RNAs evolve? *FEMS Microbiol Rev* 39(3):379–391.
15. Rutherford ST, Valastyan JS, Taillefumier T, Wingreen NS, Bassler BL (2015) Comprehensive analysis reveals how single nucleotides contribute to noncoding RNA function in bacterial quorum sensing. *Proc Natl Acad Sci USA* 112(44):E6038–E6047.
16. Chao Y, Papenfort K, Reinhardt R, Sharma CM, Vogel J (2012) An atlas of Hfq-bound transcripts reveals 3′ UTRs as a genomic reservoir of regulatory small RNAs. *EMBO J* 31(20):4005–4019.
17. Tree JJ, Granneman S, McAteer SP, Tollervey D, Gally DL (2014) Identification of bacteriophage-encoded anti-sRNAs in pathogenic Escherichia coli. *Mol Cell* 55(2):199–213.
18. Jørgensen MG, Thomason MK, Havelund J, Valentin-Hansen P, Storz G (2013) Dual function of the McaS small RNA in controlling biofilm formation. *Genes Dev* 27(10):1132–1145.
19. Romeo T, Vakulskas CA, Babitzke P (2013) Post-transcriptional regulation on a global scale: Form and function of Csr/Rsm systems. *Environ Microbiol* 15(2):313–324.
20. Göpel Y, Papenfort K, Reichenbach B, Vogel J, Görke B (2013) Targeted decay of a regulatory small RNA by an adaptor protein for RNase E and counteraction by an anti-adaptor RNA. *Genes Dev* 27(5):552–564.
21. Westermann AJ, et al. (2016) Dual RNA-seq unveils noncoding RNA functions in host-pathogen interactions. *Nature* 529(7587):496–501.
22. Holmqvist E, et al. (2016) Global RNA recognition patterns of post-transcriptional regulators Hfq and CsrA revealed by UV crosslinking in vivo. *EMBO J* 35(9):991–1011.
23. Sharma CM, et al. (2010) The primary transcriptome of the major human pathogen Helicobacter pylori. *Nature* 464(7286):250–255.
24. Georg J, Hess WR (2011) cis-antisense RNA, another level of gene regulation in bacteria. *Microbiol Mol Biol Rev* 75(2):286–300.
25. Erickson HP (2009) Size and shape of protein molecules at the nanometer level determined by sedimentation, gel filtration, and electron microscopy. *Biol Proced Online* 11:32–51.
26. Rederstorff M, et al. (2010) RNPomics: Defining the ncRNA transcriptome by cDNA library generation from ribonucleo-protein particles. *Nucleic Acids Res* 38(10):e113.
27. Wassarman KM, Storz G (2000) 6S RNA regulates E. coli RNA polymerase activity. *Cell* 101(6):613–623.
28. Giudice E, Macé K, Gillet R (2014) Trans-translation exposed: Understanding the structures and functions of tmRNA-SmpB. *Front Microbiol* 5:113.
29. Miyakoshi M, Chao Y, Vogel J (2015) Regulatory small RNAs from the 3′ regions of bacterial mRNAs. *Curr Opin Microbiol* 24:132–139.
30. Said N, et al. (2009) In vivo expression and purification of aptamer-tagged small RNA regulators. *Nucleic Acids Res* 37(20):e133.
31. Kunte HJ, Crane RA, Culham DE, Richmond D, Wood JM (1999) Protein ProQ influences osmotic activation of compatible solute transporter ProP in Escherichia coli K-12. *J Bacteriol* 181(5):1537–1543.
32. Chaulk SG, et al. (2011) ProQ is an RNA chaperone that controls ProP levels in Escherichia coli. *Biochemistry* 50(15):3095–3106.
33. Li GW, Burkhardt D, Gross C, Weissman JS (2014) Quantifying absolute protein synthesis rates reveals principles underlying allocation of cellular resources. *Cell* 157(3):624–635.
34. Sheidy DT, Zielke RA (2013) Analysis and expansion of the role of the Escherichia coli protein ProQ. *PLoS One* 8(10):e79656.
35. Silva IJ, Ortega AD, Viegas SC, García-Del Portillo F, Arraiano CM (2013) An RpoS-dependent sRNA regulates the expression of a chaperone involved in protein folding. *RNA* 19(9):1253–1265.
36. Lalaouna D, et al. (2015) A 3′ external transcribed spacer in a tRNA transcript acts as a sponge for small RNAs to prevent transcriptional noise. *Mol Cell* 58(3):393–405.
37. Han K, Kim KS, Bak G, Park H, Lee Y (2010) Recognition and discrimination of target mRNAs by Sib RNAs, a cis-encoded sRNA family. *Nucleic Acids Res* 38(17):5851–5866.
38. van Biesen T, Frost LS (1994) The FinO protein of IncF plasmids binds FinP antisense RNA and its target, traJ mRNA, and promotes duplex formation. *Mol Microbiol* 14(3):427–436.
39. Dubey AK, Baker CS, Romeo T, Babitzke P (2005) RNA sequence and secondary structure participate in high-affinity CsrA-RNA interaction. *RNA* 11(10):1579–1587.
40. Jerome LJ, van Biesen T, Frost LS (1999) Degradation of FinP antisense RNA from F-like plasmids: The RNA-binding protein, FinO, protects FinP from ribonuclease E. *J Mol Biol* 285(4):1457–1473.
41. Brown CT, et al. (2015) Unusual biology across a group comprising more than 15% of domain bacteria. *Nature* 523(7559):208–211.
42. Weinberg Z, Perreault J, Meyer MM, Breaker RR (2009) Exceptional structured noncoding RNAs revealed by bacterial metagenome analysis. *Nature* 462(7273):656–659.
43. Ingolia NT, Ghaemmaghami S, Newman JR, Weissman JS (2009) Genome-wide analysis in vivo of translation with nucleotide resolution using ribosome profiling. *Science* 324(5924):218–223.
44. Castello A, et al. (2012) Insights into RNA biology from an atlas of mammalian mRNA-binding proteins. *Cell* 149(6):1393–1406.
45. Baltz AG, et al. (2012) The mRNA-bound proteome and its global occupancy profile on protein-coding transcripts. *Mol Cell* 46(5):674–690.
46. Attaiech L, et al. (2016) Silencing of natural transformation by an RNA chaperone and a multitarget small RNA. *Proc Natl Acad Sci USA* 113(31):8813–8818.
47. Förstner KU, Vogel J, Sharma CM (2014) READemption-a tool for the computational analysis of deep-sequencing-based transcriptome data. *Bioinformatics* 30(23):3421–3423.

SUPPORTING INFORMATION

Grad-seq guides the discovery of ProQ as a major small RNA binding protein

Alexandre Smirnov[1], Konrad U. Förstner[1,2], Erik Holmqvist[1], Andreas Otto[3], Regina Günster[1], Dörte Becher[3], Richard Reinhardt[4], Jörg Vogel[1]*

[1]RNA Biology Group, Institute of Molecular Infection Biology, University of Würzburg, Josef-Schneider-Straße 2, D-97080 Würzburg, Germany;

[2]Core Unit Systems Medicine, University of Würzburg, Josef-Schneider-Straße 2, D-97080 Würzburg, Germany;

[3]Institute for Microbiology, University of Greifswald, D-17489 Greifswald, Germany;

[4]Max Planck Genome Centre Cologne, MPI for Plant Breeding Research, D-50829 Cologne, Germany

*Correspondence to: Jörg Vogel, RNA Biology Group, Institute for Molecular Infection Biology, University of Würzburg, Josef-Schneider-Straße 2, D-97080 Würzburg, Germany; +49-931-3182-575, joerg.vogel@uni-wuerzburg.de

SI Materials and Methods

Bacteria and media

For all experiments, *Salmonella enterica enterica* serovar Typhimurium SL1344 (see the complete list of strains in Tables S2 and S3) were streaked on LB plates with appropriate antibiotics and grown overnight at 37°C. Individual colonies were inoculated in liquid LB medium with the same antibiotics for subculturing overnight at 37°C with shaking at 220 rpm, and then diluted 1:100 in fresh LB medium with antibiotics for culturing to the desired density (exponential phase – OD_{600} = 0.5, transition phase – OD_{600} = 2, stationary phase – 6 h after the culture reached OD_{600} = 2).

Deletion and FLAG-tagged strains were generated as described in (1, 2) with the use of gene-specific oligonucleotides (Tables S2 and S3). All initial deletion strains were transduced into fresh WT background with the use of P22 phage, and the kanamycin resistance cassettes were removed by pCP20 transformation to avoid polar effects, as described in (1). The *proQ* deletion removes most of the ORF (including the initiator codon) without disrupting the internal *prc* promoter (3).

For total RNA sample preparation, 4 OD_{600} of culture were mixed with 1/5 volume of the 95% ethanol, 5% phenol, snap-frozen in liquid nitrogen and thawed on ice, and RNA was extracted with the TriZOL reagent (Life Technologies). For total protein preparation, 0.4-0.5 OD_{600} of culture were pulse-pelleted and the cell pellet was resuspended in 100 µl 1×Laemmli buffer.

Protein gel electrophoresis and Western blotting

Protein samples were resolved by 12% SDS-PAGE followed by Coomassie staining. For Western blotting, 15% SDS-PAGE was used, followed by semi-dry transfer on nitrocellulose membranes and probing with protein-specific antisera. FLAG-tagged proteins were detected with monoclonal anti-FLAG antibodies (Sigma, #F1804). Antisera for ribosomal proteins, ProQ, MukB/RNase E are kind gifts of Matthias Springer, Daniel Sheidy, and Agamemnon Carpousis, respectively. GroEL was detected with commercial antibodies (Sigma G6532).

RNA gel electrophoresis and Northern blotting

RNA samples were resolved by 8% PAGE in 1×TBE and 7M urea and stained with ethidium bromide and/or transferred onto a Hybond+ membrane (GE Healthcare Life Sciences) and probed with RNA-specific oligonucleotides (Table S3). 5S rRNA was probed for as a loading control.

Glycerol gradient fractionation

For lysis, 200 OD_{600} of JVS-01338 (*hfq-3×FLAG*) bacterial culture grown to OD_{600}=2 (transition phase) were harvested by centrifugation at 4000 g at 4°C for 15 min, washed thrice with ice-cold 1×TBS and resuspended in 500 µl of the lysis buffer (20 mM Tris-HCl, pH7.5, 150 mM KCl, 1 mM $MgCl_2$, 1 mM DTT, 1 mM PMSF, 0.2% Triton X100, 20 U/ml DNase I, Thermo Scientific, 200 U/ml SUPERase-IN, Life Technologies). Lysis was carried out on a Retsch MM400 machine at 30 Hz for 10 min in the presence of 750 µl 0.1 mm glass beads (BioSpec Products). The lysate was cleared by centrifugation at 14,000 g at 4°C for 10 min and layered on a linear 10%-40% (w/v) glycerol gradient in the same buffer without DNase I nor SUPERase-IN, formed in a Beckman SW40Ti

tube with the use of the Gradient Station model 153 (Biocomp). The gradient was centrifuged at 100,000 g (23,700 rpm) for 17 h at 4°C and fractionated in 20 equal fractions by pipetting. OD_{260} for each fraction was measured with Nanodrop. For protein analysis, 90 µl of each fraction were mixed with 30 µl of the 5× Laemmli loading buffer (for the pellet, 20 µl per 30 µl of Laemmli buffer were taken). Samples were stored at -20°C. For RNA isolation, the rest of each fraction was deproteinized by addition of 1% SDS and 1 volume of hot phenol and shaking at 1,500 rpm at 55°C for 5 min. Phases were separated by centrifugation at 12,000 g for 15 min at 4°C. The aqueous phases were added glycogen to 50 µg/ml and RNA was precipitated with 60% isopropanol. The RNA pellets were dissolved in 35 µl of DEPC-treated sterile MilliQ water and stored at -80°C.

RNA-seq

For Grad-seq, two biological replicates have been analyzed. 85 pg/µl of the spike-in RNA (5'P-CUCGUCCGACGUCACCUAGA, IBA) had been added to each fraction prior the library preparation. RNA-seq libraries were prepared by Vertis AG (Freising-Weihenstephan, Germany). Briefly, RNA was polyadenylated with poly(A) polymerase, 5'-triphosphates were removed with tobacco acid pyrophosphatase followed by ligation of a 5'-adapter. First-strand cDNA synthesis was performed with the use of an oligo(dT) barcoded adapter primer and the M-MVL reverse transcriptase. The resulting cDNA was PCR-amplified with a high fidelity DNA polymerase. cDNA was purified with the Agencourt AMPure XP kit (Beckman Coulter Genomics) and sequenced on an Illumina HiSeq2000 platform. The resulting reads were mapped to the S. Typhimurium SL1344 genome with the use of the READemption pipeline version 0.3.4 (4).

For in-gradient profiling, fraction-wise gene-specific RNA-seq read counts were normalized by corresponding spike-in counts. For few fractions, biases uniformly distorting all

profiles were evident: those were manually readjusted which allowed reconstitution of smooth profiles. To compare shapes of distributions by PCA, all profiles with ≥30 reads in at least one fraction were power-transformed to improve linearity and standardized to the range from 0 to 1. To derive averaged distributions for RNA classes, profiles of individual ncRNAs were standardized to the range from 0 to 1, summed up and averaged fraction-wise. For PCA, RNA profiles were power-adjusted to improve linearity (the exponent value – 0.8268 - was derived from the regression analysis of RNA mass vs spike-in reads fraction-wise). PCA was performed in R and visualized in R and Python. For sRNAs, PC1 (~44% of variance) mostly reflects the influence of few mRNA-derived and/or mRNA-overlapping sRNAs (following, like mRNAs, strong ribosomal components) and, therefore, is uninformative for our purpose of revealing groups of noncoding RNAs. We opted for PC2 (~22% of variance) and PC3 (~13% of variance) analysis instead, which allowed a better resolution and clustering of typical sRNAs. Both PC1 vs PC2 and PC2 vs PC3 plots are available on Figs S4. All molecular weight estimates provided in this work were made assuming a most frequently encountered moderately elongated shape of particles (5).

RNA-seq data are available in Gene Expression Omnibus (accession number GSE62988). The workflow implemented as Shell script and the analysis-specific tools are deposited at Zenodo at DOI:10.5281/zenodo.35176.

Affinity chromatography of MS2 aptamer-tagged sRNAs

Affinity chromatography was performed on cell lysates from *Salmonella* cultures grown to the transition phase as described in (6) with addition of *in vitro* transcribed MS2-aptamer-tagged sRNAs. Templates for the latter were created by overlapping PCR with sRNA- and MS2-specific primers (see Table S3 for a detailed description). Each sRNA was assayed at least twice, usually

with both 3'- and 5'-positioning of the MS2 tag. For each series of experiments, MS2 RNA was used as a negative control. Proteins co-purified with bait sRNAs were visualized by silver staining and identified by LC-MS/MS. Those reproducibly found in replicate experiments and absent from respective MS2 control samples were considered specific binding partners.

RNA co-immunoprecipitation

For RNA coIP, 50 OD_{600} of bacteria were grown to the desired growth stage and harvested by centrifugation. They were lysed as described in the 'Glycerol gradient fractionation' section. After clearing the lysate, the equivalent of 0.5 OD_{600} was diluted to 90 µl with 1× Laemmli buffer (lysate protein sample) and stored at -20°C. The equivalent of 5 OD_{600} was saved for RNA extraction with TriZOL (lysate RNA sample). The lysate was added 35 µl of monoclonal anti-FLAG M2 antibody (Sigma, #F1804) and rocked for 30 min at 4°C. Then 75 µl of prewashed Protein A sepharose (Sigma, #P6649) were added and the mixture was rocked for additional 30 min. Afterwards, beads were washed extensively with the lysis buffer, and similar flow-through and wash protein and RNA samples were collected. Beads were resuspended in the lysis buffer, mixed with an equal volume of phenol:chloroform:isoamyl alcohol (25:24:1, pH4.5, Roth) for 20 s and incubated at room temperature for 3 min. After centrifugation, the aqueous phase was precipitated with isopropanol (coIP RNA sample) and the organic phase was precipitated with acetone (coIP protein sample). The purified RNA samples were treated with DNase I (Thermo Scientific) to remove the residual DNA and reisolated with phenol:chloroform:isoamyl alcohol. The protein coIP samples were soaked in 1× Laemmli buffer and denatured at 95°C for 10 min. For Western blotting, the equivalents of 0.05 OD_{600} (for lysate, flow-through and wash samples) or 5 OD_{600} (for coIP samples) were loaded on the gel. For Northern blotting, the equivalents of 0.3 OD_{600} and 0.03 OD_{600} were analyzed, respectively. Independent RNA co-immunoprecipitation

experiments were performed in *E. coli* and in *Salmonella* in the stationary phase twice, in *Salmonella* in the exponential phase twice, in *Salmonella* in the transition phase four times, with very similar results.

Analysis of coIP enrichment data

Gene-wise read counts were normalized by the total number of mapped reads. Enrichment is then calculated as a quadruple ratio of the lysate and coIP read counts in the FLAG-tagged and WT (untagged) strains, thus accounting for both the input transcript abundance and the background nonspecific interaction with beads:

$$E = \frac{[FLAGcoIP][WTlysate]}{[FLAGlysate][WTcoIP]}$$

Only genes with at least 5 reads in each of the four samples were used for enrichment calculations. The read countings of coIP libraries and lysate libraries were compared for samples from exponential, transition and stationary growth phases in 2, 4, and 2 biological replicates, respectively (which was expected to ensure the statistical power of 0.5-0.8, based on previously reported guidelines (7)). Enrichment factors were calculated with DESeq2 (8) but using the total number of aligned reads for the normalization. Transcripts enriched with $\log_2$(enrichment) values over two medians (i.e. 0.91, 1.13, and 0.75 for exponential, transition, and stationary phases, respectively, resulting in cut-off fold-changes of 3.76-fold, 4.38-fold, and 3.36-fold, respectively.) and an FDR-adjusted *P*-value below 0.05 were declared “ProQ-bound”.

Mass spectrometry

Each sample (gradient fraction or affinity chromatography pull-down) was subjected to one-dimensional gel electrophoresis followed by LC-MS/MS analysis. We followed the protocol published in (9) with minor modifications. In brief, each of the 20 gel lanes was cut into 10 equidistant pieces and subjected to tryptic digestion. Eluted peptides were then loaded and desalted on a self-packed reversed phase C18 column using a Proxeon EasynLC II. Peptides were separated in a binary gradient of 85 minutes from 1 to 99% buffer B (0.1% (v/v) acetic acid in acetonitrile; buffer A: (0.1% (v/v) acetic acid)) with a constant flow rate of 300 nL/min. MS and MS/MS data were recorded with an LTQ Orbitrap (Thermo) coupled online to the LC- setup. Each scan cycle consisted of a survey scan with a resolution of R = 30,000 in the Orbitrap section followed by dependent scans (MS/MS) of the five most abundant precursor ions. Database searching of the MS/MS '*.raw' data was done with Sorcerer-SEQUEST (ThermoFinnigan; version v.27, rev. 11) against the *S. enterica* strain SL1344 using a target decoy protein sequence database (complete proteome set of *S. enterica* strain SL1344 with a set of common laboratory contaminants). The resulting out files were compiled with Scaffold 4. Proteins were only considered as identified if at least 2 unique peptides matching quality criteria (delta cN > 0.1 and XCorr > 2.2; 3.5; 3.75 for doubly, triply or higher charged peptides) have been identified. For sedimentation profiling of proteins in glycerol gradients, two biological replicates have been analyzed. For reconstruction of in-gradient profiles, only proteins with ≥5 spectral counts in the peaking fraction were retrieved. The raw spectral counts were then normalized by the total number of spectral counts in each fraction and multiplied by the intensity of the Coomassie staining across the corresponding lane. The mass spectrometry proteomics data are deposited to the ProteomeXchange Consortium via the PRIDE partner repository (dataset identifier PXD003360).

ProQ purification and electrophoretic mobility shift assay (EMSA)

The S. Typhimurium *proQ* gene was cloned into pTYB11 plasmid (NEB) to allow the intein-based expression and purification (IMPACT) of a tagless protein, as described in the manufacturer's protocol. For EMSA, 5 nM ^{32}P-5'-end labeled *in vitro* transcribed RNA (MEGAscript T7 transcription kit, Life Technologies) were incubated with varying concentrations of ProQ (5 nM to 1 μM) in the reaction buffer (25 mM Tris-HCl, pH7.4, 100 mM NaCl, 1 mM $MgCl_2$) at 37°C for 20 min. After binding, the samples were resolved by native 8% PAGE in 0.5× TBE at 4°C, the gel was vacuum-dried and bands were visualized with Phosphorimager. Apparent K_d values were estimated with the Scatchard procedure which accounts for partial inactivation of the protein. For competition assays, 1-1,000-fold molar excess of yeast tRNA (LifeTechnologies) or the same cold RNA were used as nonspecific and specific competitors, respectively.

RNA-seq analysis of ΔproQ

For total RNA sequencing, RNA samples from WT carrying the empty pJV300 plasmid, Δ*proQ* strain carrying the empty pJV300 plasmid, and Δ*proQ* strain complemented with a pZE12-proQ plasmid (n = 3 for each strain, which was expected to ensure the statistical power of ~0.7, based on previously reported guidelines (7)) were collected at OD_{600} = 2, as described above. cDNA preparation, RNA-seq and read mapping were performed as described in the 'RNA-seq' section. Gene expression changes were analyzed with RUV-edgeR (10) to account for nonuniform RNA fragmentation across replicates during cDNA library generation.

RNA in vivo stability assay

Bacterial cultures were grown in a water bath to the stationary phase, added 500 μg/ml rifampicin, and 4 OD_{600} samples were collected 0, 1, 2, 4, 8, 16, and 32 min later. Each sample was immediately mixed with 1/5 volume of 95% ethanol and 5% phenol and frozen in liquid nitrogen. RNA was isolated with TriZOL (Life Technologies) and analyzed by Northern blotting with the use of ImageQuant Tools. 5S rRNA was used as loading control.

Statistical and other analyses

Most descriptive statistical analyses have been performed in Excel. Most statistical tests used in this work are nonparametric to avoid the assumptions of normal distribution and homoscedasticity, with big sample sizes ensuring adequate statistical power. Fisher's exact test was done with the use of GraphPad QuickCalcs (www.graphpad.com/quickcalcs/). Mann-Whitney test, Pearson's and Spearman's correlations and regression analysis were carried out with the use of Free Statistics and Forecasting Software v1.1.23-r7 (11). Wilcoxon matched-pairs signed-ranks test calculator is available on http://www.fon.hum.uva.nl/Service/ank_Test.html. Kolmogorov-Smirnov test is performed with Statistics to use (12). All tests were two-sided. KEGG enrichment analysis was performed with the R. package "clusterProfiler".

Multiple alignment of selected sequences of the ProQ/FinO family was carried out with COBALT (13). It included the following species: γ-proteobacteria - *ECO* FinO, *Escherichia coli* FinO, *ECO* ProQ, *Escherichia coli* ProQ, *SEN*, *Salmonella enterica* ProQ, *VCH*, *Vibrio cholerae* ProQ, *LPN*, *Legionella pneumophila* ProQ, *MRH*, *Marinobacterium rhizophilum* ProQ, *SAM, Succinomonas amylolytica* ProQ, Phage ΦEa104, *Erwinia* phage phiEa104 FinO-like protein; α-proteobacteria – *SME, Sinorhizobium meliloti* FinO-like protein, *MAL, Mesorhizobium alhagi* FinO-like protein, *AFE,*

Afipia felis FinO-like protein, *OTH*, Candidatus *Odyssella thessalonicensis* FinO-like protein; β-proteobacteria – *BVI, B. vietnamiensis* ProQ, *NME, Neisseria meningitidis* 1681 (14).

The aligned sequences of the ProQ/FinO family proteins (InterPro IPR016103) were downloaded from PFAM and redundant sequences removed. Based on this non-redundant alignment a phylogenetic tree was constructed with the use of PhyML (with 600 bootstraps rounds), Phylip (Version 3.2), Cladisitics 5, and Clann (15). The resulting tree in Newick format was visualized using iTOL (16).

Predictions of RNA secondary structures are done with *RNAfold* (17). For analyses shown in Fig. S9E,F, only sRNAs with well-defined termini were retained, which was necessary for high-confidence folding energy predictions. This criterion was pre-established.

SI figures

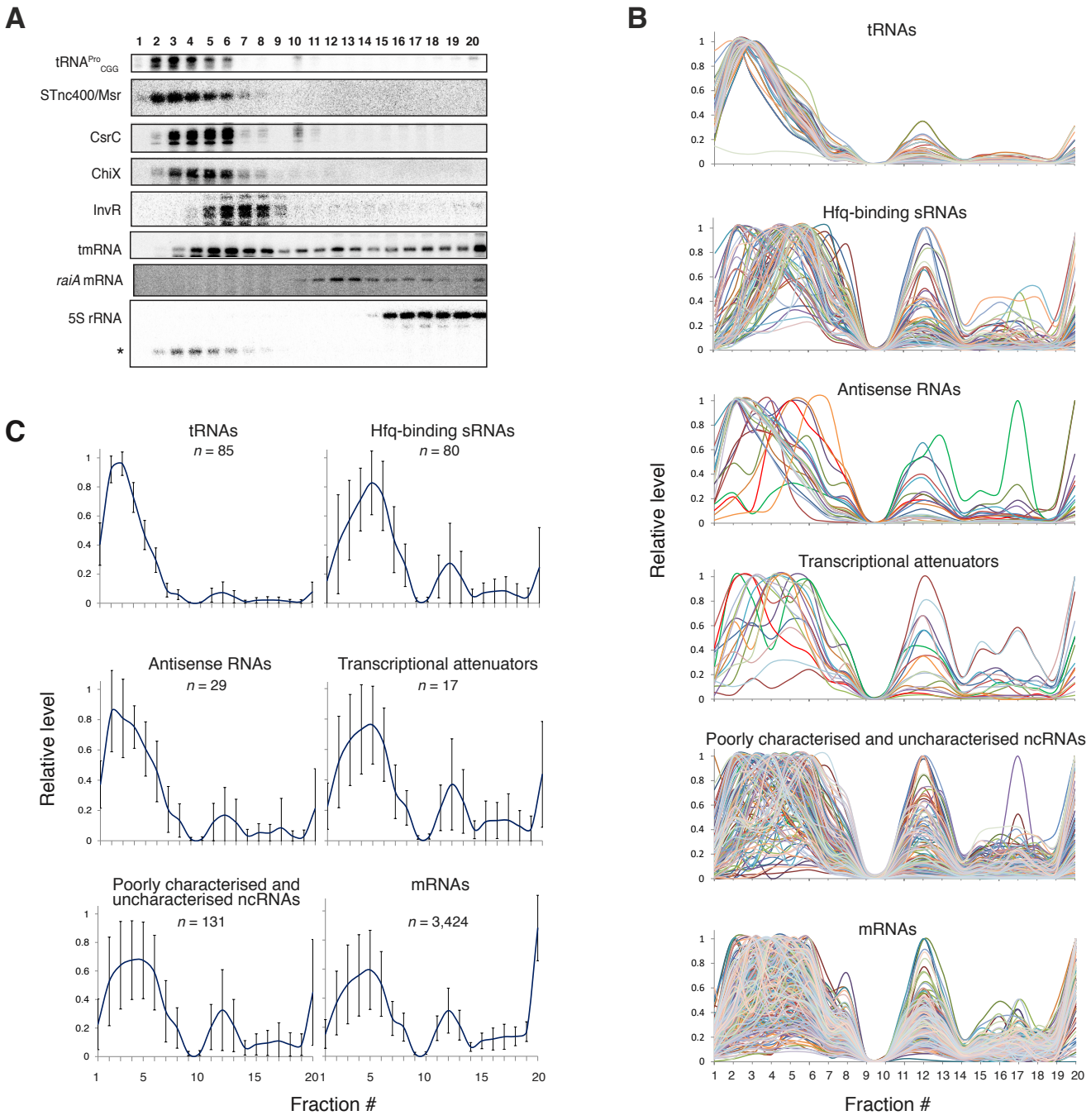

Figure S1. Grad-seq profiles reveal diverse biochemical behavior of bacterial RNA classes. (A) Northern blots of samples shown on Figs. 1 and S3 probed with RNA-specific oligonucleotides. Retron-encoded STnc400/Msr, CsrA-sequestering CsrC, Hfq-dependent ChiX and InvR, and tmRNA represent different groups of bacterial ncRNAs. A subpopulation of 5S rRNA not assembled into 50S ribosomal subunits is marked with an asterisk. **(B)** Grad-seq in-gradient distributions of major known bacterial RNA classes, as determined by RNA-seq (all profiles are standardized to the range from 0 to 1). **(C)** Averaged Grad-seq profiles of major known *Salmonella* RNA classes. All individual profiles of RNAs from each class were cumulated and presented as an average along the gradient ±SD.

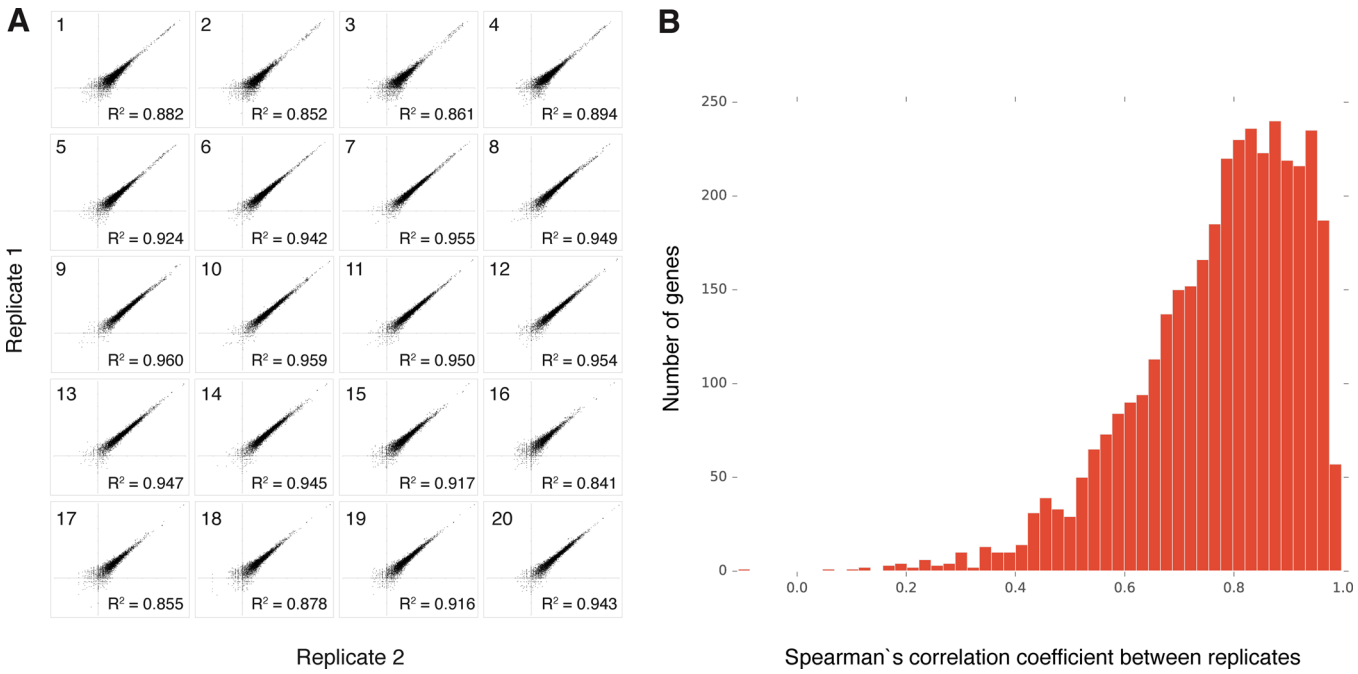

Figure S2. Evaluation of Grad-seq reproducibility. (A) Fraction-wise reproducibility of RNA-seq data used for reconstruction of Grad-seq RNA distributions. Pearson's determination coefficients are computed on log-transformed RNA-seq read counts for two biological gradient replicates. **(B)** Distribution of Spearman's correlation coefficients of individual Grad-seq profiles between the two replicates. All individual profiles of RNAs from each class were cumulated and presented as an average along the gradient ±SD.

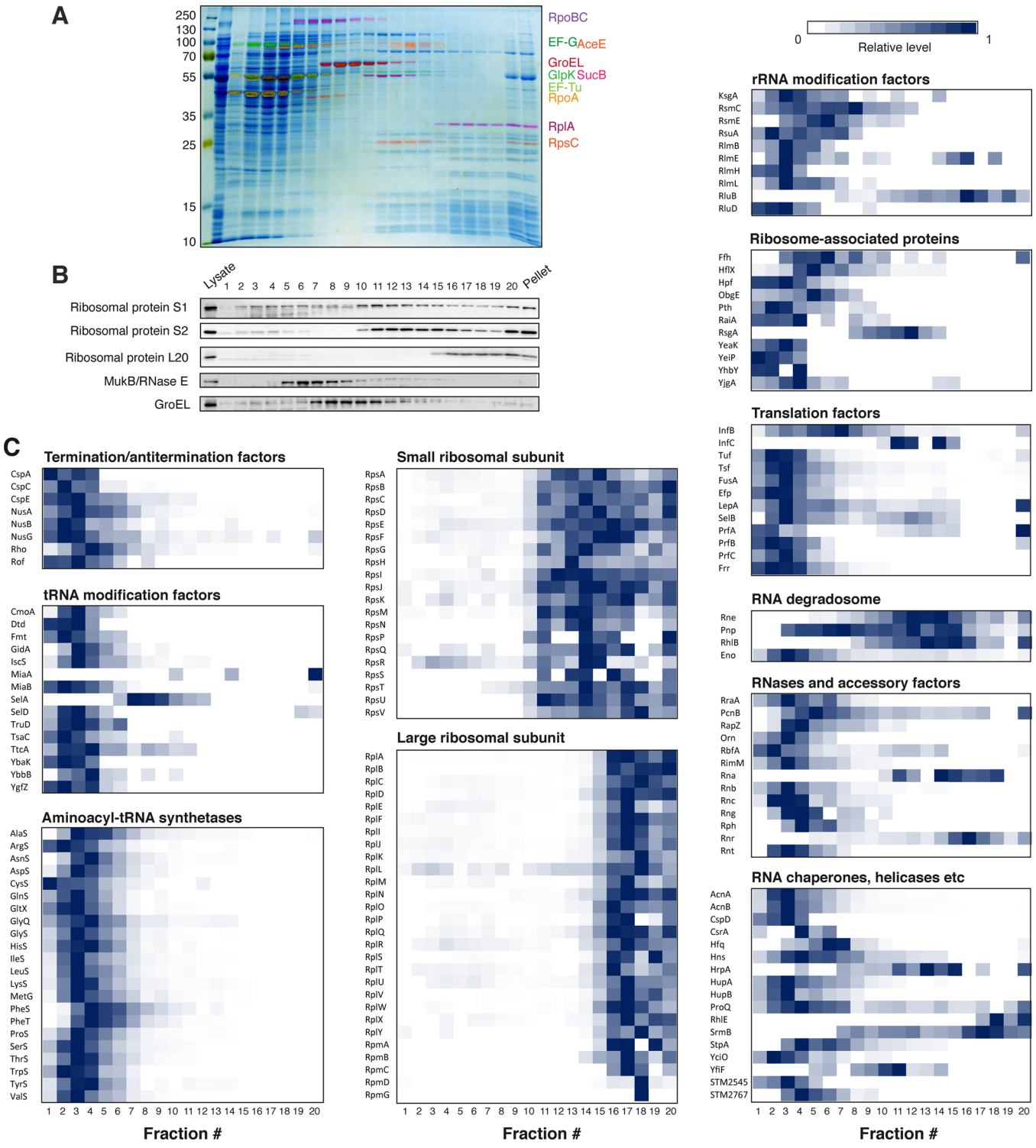

Figure S3. Complexes formed by Salmonella proteins as visualized by glycerol gradient sedimentation followed by mass-spectrometric analysis of fractions. (A,B) Distributions of major *Salmonella* proteins in a glycerol gradient analyzed by conventional techniques. *Salmonella* Typhimurium SL1344 cells grown to the transition phase were lysed and natively resolved on a 10-40% glycerol gradient. Fractions are numbered from the top to the bottom of the gradient. **(A)** Coomassie-stained SDS gel showing the protein profile of the gradient. Selected bands identified with LC-MS/MS are highlighted in false color and identified on the right. The ladder (in kDa) is shown on the left. **(B)** Western blots of samples shown on panel (A) probed with protein-specific antisera. **(C)** In-gradient distributions of major groups of known and putative RBPs, their complexes and associated factors, as determined by LC-MS/MS. All profiles are standardized to the range from 0 to 1.

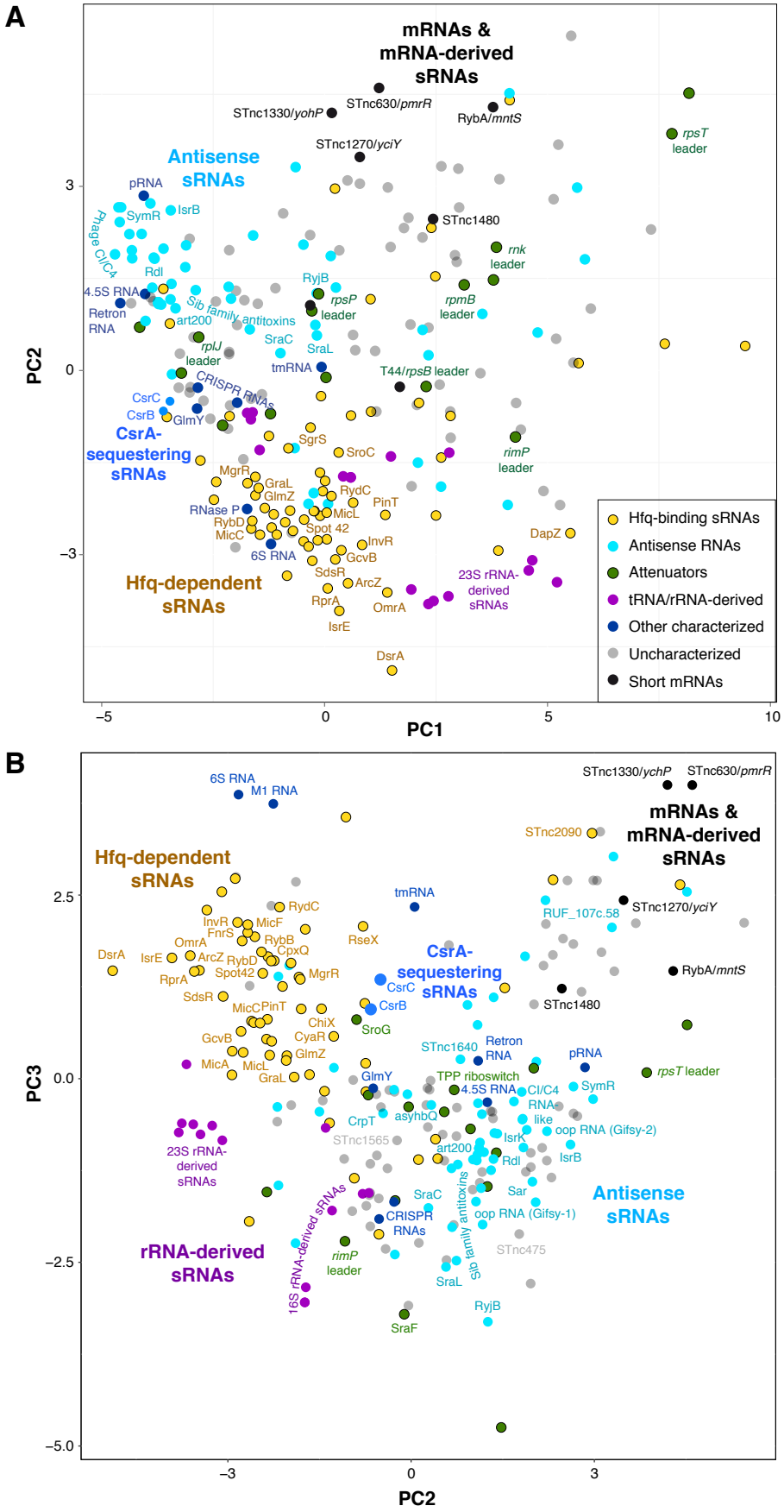

Figure S4. Principal component analyses (PCA) of Grad-seq profiles of *Salmonella* sRNAs. Grad-seq PCA plots of 238 *Salmonella* sRNAs with detailed annotation. PC1 (~44% of variance) vs PC2 (~22% of variance, panel A) and PC2 vs PC3 (~13% of variance, panel B) plots are shown.

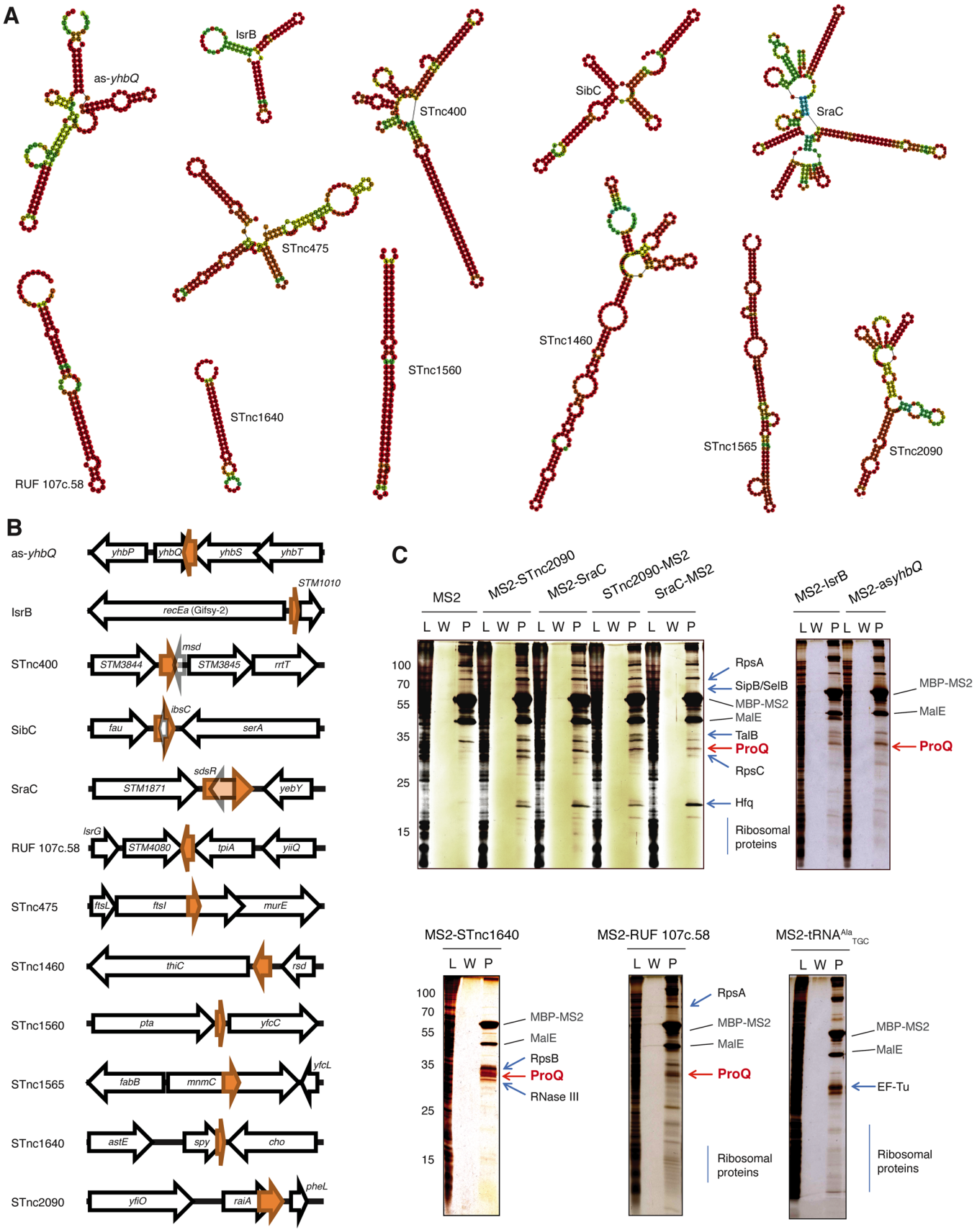

Figure S5. Pull-down of protein partners interacting with select unusually distributed MS2 aptamer-tagged sRNAs from *Salmonella* cell lysates. (A,B) Predicted secondary structures (panel A) and the genomic context (panel B) of the selected sRNAs (orange arrows). **(C)** Examples of affinity chromatography experiments. Lysate (L), wash (W) and pull-down (P) fractions are resolved on SDS gels and silver-stained. Specific protein bands which were not observed in MS2 aptamer controls are identified by LC-MS/MS. MBP-MS2 is maltose-binding protein fused with the MS2 phage coat protein, MalE is the endogenous maltose-binding protein. The upper left panel presents experiments with both 5'- and 3'-MS2-tagged sRNAs. tRNA on the bottom right panel is shown as an additional control. Ladder (in kDa) is shown on the left.

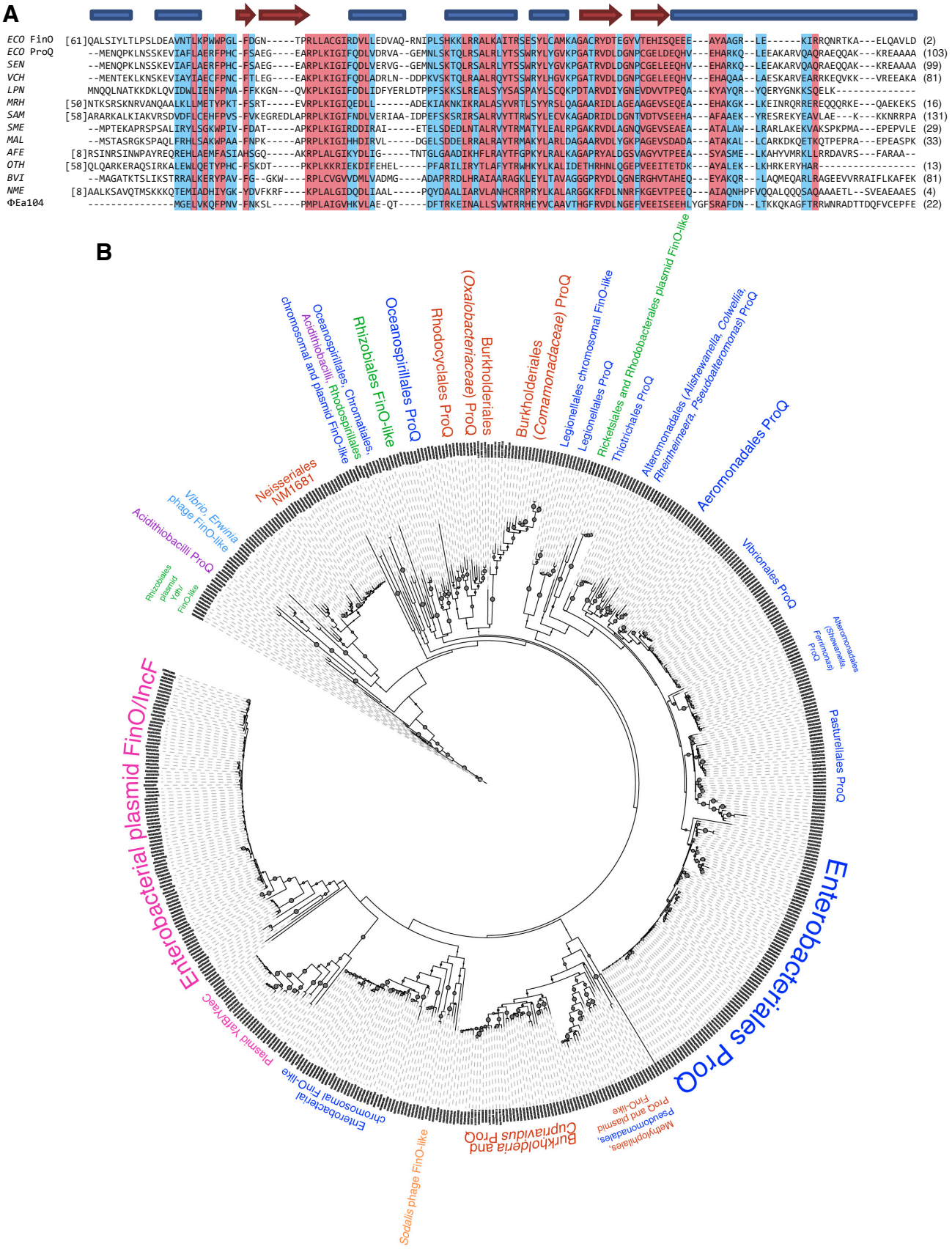

Figure S6. ProQ/FinO protein family. (A) Alignment of FinO-like domains of selected members of the ProQ/FinO family from various proteobacteria (see SI Materials and Methods for further detail). Conserved residues are red, no-gap positions are blue. FinO structural elements (α-helices: blue boxes, β-sheets: red arrows) are mapped according to (18). **(B)** Phylogenetic tree of known representatives of the ProQ/FinO family. α-, β-, γ-proteobacteria and Acidithiobacilli groups are shown in blue, red, green and purple, respectively. Other colors are used to highlight diverse plasmid- and phage-encoded members found in γ-proteobacteria (mostly enterobacteria).

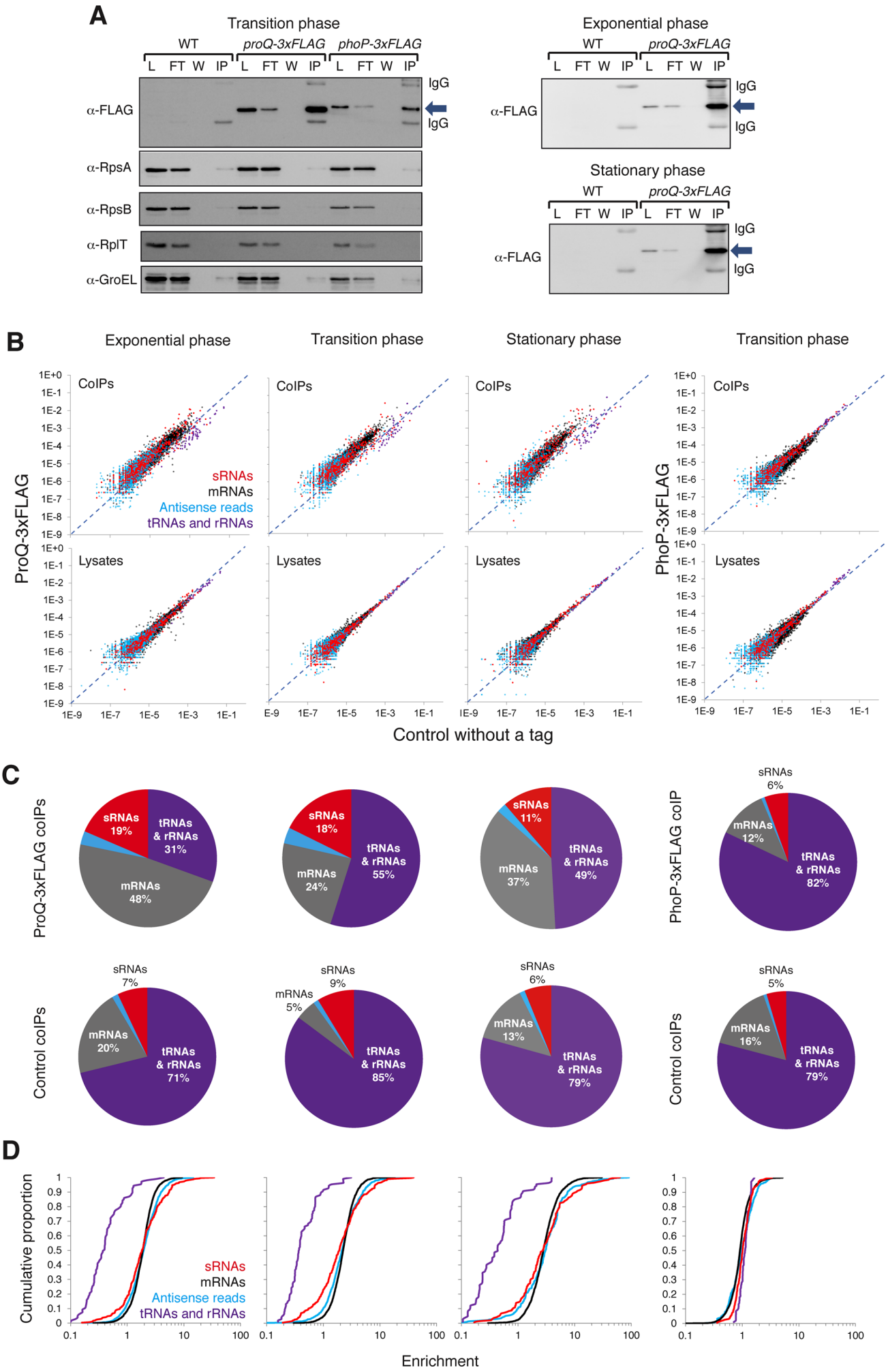
A
Transition phase
WT
proQ-3xFLAG
phoP-3xFLAG
L FT W IP L FT W IP L FT W IP
α-FLAG
α-RpsA
α-RpsB
α-RplT
α-GroEL
IgG
IgG
Exponential phase
WT
proQ-3xFLAG
L FT W IP L FT W IP
α-FLAG
IgG
IgG
Stationary phase
WT
proQ-3xFLAG
L FT W IP L FT W IP
α-FLAG
IgG
IgG
B
Exponential phase
Transition phase
Stationary phase
Transition phase
CoIPs
Lysates
sRNAs
mRNAs
Antisense reads
tRNAs and rRNAs
ProQ-3xFLAG
PhoP-3xFLAG
Control without a tag
C
ProQ-3xFLAG coIPs
sRNAs 19%
tRNAs & rRNAs 31%
mRNAs 48%
sRNAs 18%
tRNAs & rRNAs 55%
mRNAs 24%
sRNAs 11%
tRNAs & rRNAs 49%
mRNAs 37%
PhoP-3xFLAG coIP
sRNAs 6%
mRNAs 12%
tRNAs & rRNAs 82%
Control coIPs
sRNAs 7%
mRNAs 20%
tRNAs & rRNAs 71%
sRNAs 9%
mRNAs 5%
tRNAs & rRNAs 85%
sRNAs 6%
mRNAs 13%
tRNAs & rRNAs 79%
Control coIPs
sRNAs 5%
mRNAs 16%
tRNAs & rRNAs 79%
D
Cumulative proportion
sRNAs
mRNAs
Antisense reads
tRNAs and rRNAs
Enrichment

Figure S7. ProQ is a global RNA-binding protein. Co-immunoprecipitation of *Salmonella* ProQ-associated RNAs. **(A)** Chromosomally FLAG-tagged ProQ (blue arrow) was detected on Western blot with FLAG-specific antibodies in lysate (L), flow-through (FT), wash (W) and immunoprecipitation (IP) fractions. An untagged WT strain and a strain with a chromosomally FLAG-tagged DNA-binding protein, PhoP, were used as negative controls. The absence of contamination with other abundant proteins was verified with specific antisera. **(B)** Normalized read counts before (Lysates) and after (coIPs) pull-downs performed in three growth phases are plotted versus WT negative control. **(C)** Read distributions between RNA classes in ProQ-3×FLAG, PhoP-3×FLAG and WT control coIPs for the corresponding experiments. **(D)** Cumulative enrichment distributions for the corresponding experiments. The figure shows representatives of at least two independent experiments in each growth phase.

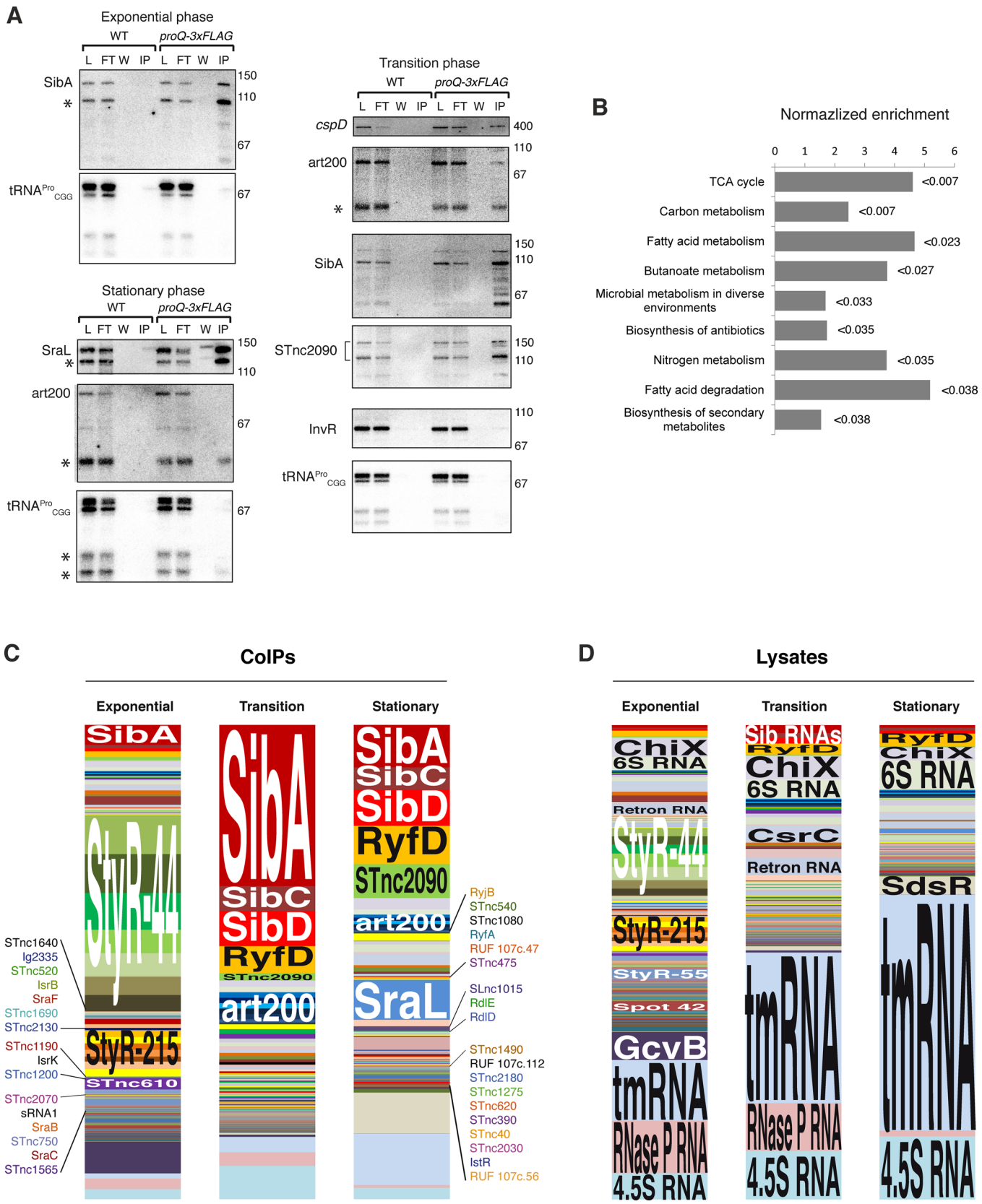

Figure S8. Diversity of ProQ-binding RNAs revealed by RNA co-immunoprecipitation. (A) Northern blot detection of ProQ-associated RNAs in co-immunoprecipitation experiments shown in Fig. S7. RNA was isolated from lysate (L), flow-through (FT), wash (W) and immunoprecipitation (IP) fractions. Noncoding RNAs SibA, SraL, art200 and STnc2090 as well as the *cspD* mRNA are top ProQ targets. An Hfq-dependent sRNA, InvR, and a tRNA are shown here as examples of non-enriched transcripts. Stable RNA fragments are marked with asterisks. The positions of size markers (in nt) are shown on the right of each blot. **(B)** KEGG enrichment analysis of the mRNAs co-immunoprecipitated with ProQ. Adjusted *P*-values are provided on the right of each category. Only significantly enriched pathways (FDR < 0.05, $P_{adj} < 0.05$) are shown. **(C)** Dynamics of the noncoding ProQ interactome over growth. The chart shows sRNA read distributions in ProQ coIPs over three growth phases in *Salmonella*. StyR-44 and StyR-215 are families of ncRNAs derived from rRNA operons. art200 is a family of IS200 transposon-derived antisense RNAs. SibACD are antitoxins in Sib/*ibs* type I toxin-antitoxin systems. **(D)** sRNA read distributions in the corresponding lysates. Most prominent sRNAs are named. sRNAs are plotted in the same order in all columns on panels (B) and (C).

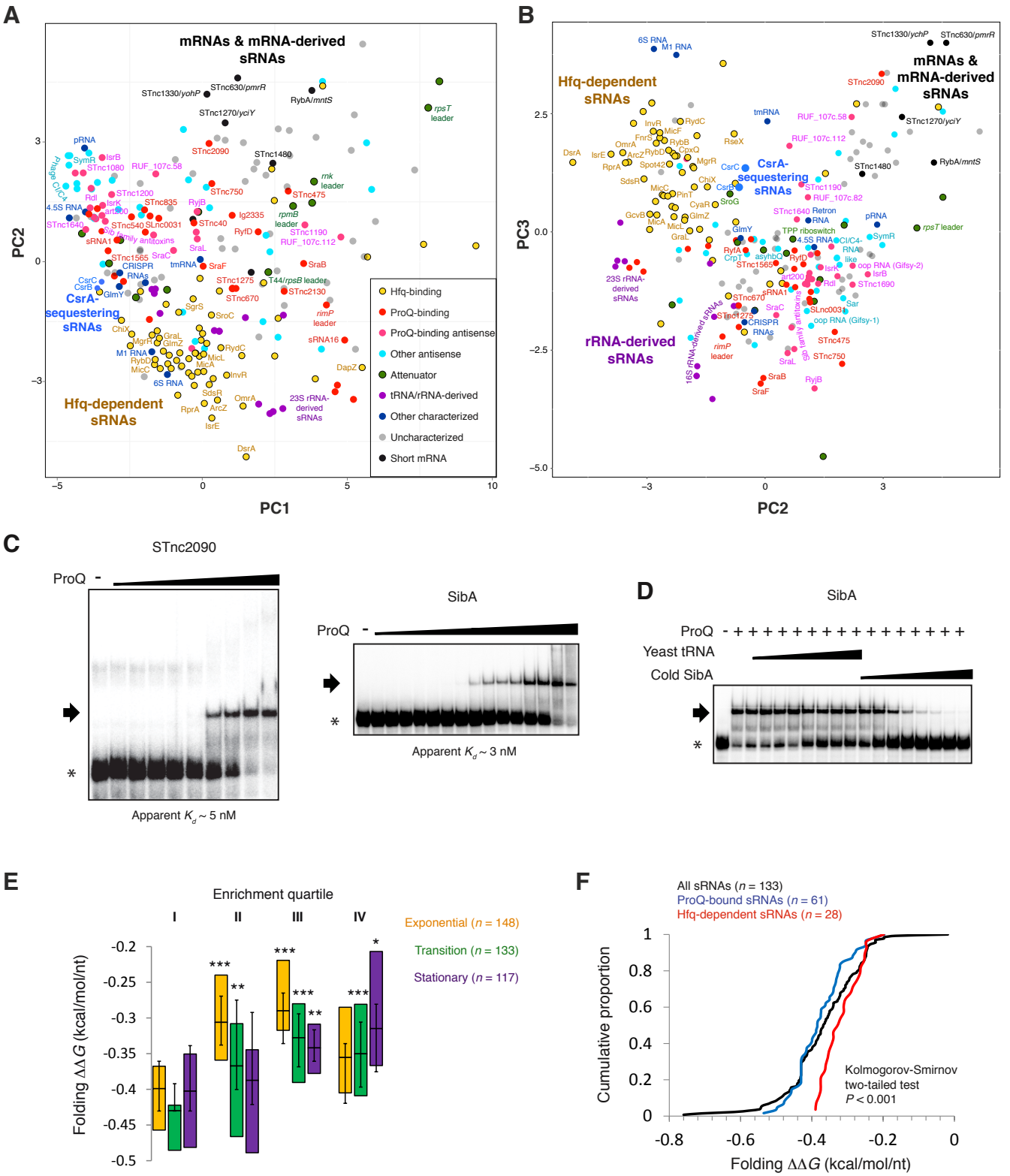

Figure S9. ProQ-interacting sRNAs form a distinct class of highly structured transcripts. (A,B) Grad-seq PCA of 238 *Salmonella* sRNAs showing the group of ProQ-associated RNAs with detailed annotation on PC1 vs PC2 (panel A) and PC2 vs PC3 (panel B) plots (cf. Figs. 4C and S4). **(C)** EMSAs performed with purified ProQ (0-1,000 nM) and two of its highly enriched ligands. Asterisks and arrows mark free RNA and ProQ-RNA complexes, respectively. Apparent K_d values were estimated by Scatchard procedure. **(D)** Competition assay of the ProQ-SibA complex with yeast tRNA and cold SibA (0-1,000-fold molar excess) as a nonspecific and a specific competitor, respectively. **(E)** ProQ prefers structured RNAs. Shown are the median predicted thermodynamic ensemble free energies of folding (normalized by the transcript length), interquartile ranges (boxes) and approximate 95% CIs of the medians (whiskers) for sRNAs binned by enrichment quartiles in three growth phases (I corresponds to most highly enriched species, IV groups worst binders). * P = 0.08, ** P < 0.04, *** P < 0.003 (Mann-Whitney test, FDR-adjusted, all comparisons with quartile I). **(F)** ProQ-associated sRNAs are significantly more structured than Hfq-dependent sRNAs. Cumulative distributions of predicted length-normalized thermodynamic ensemble folding free energies for sRNA groups are shown.

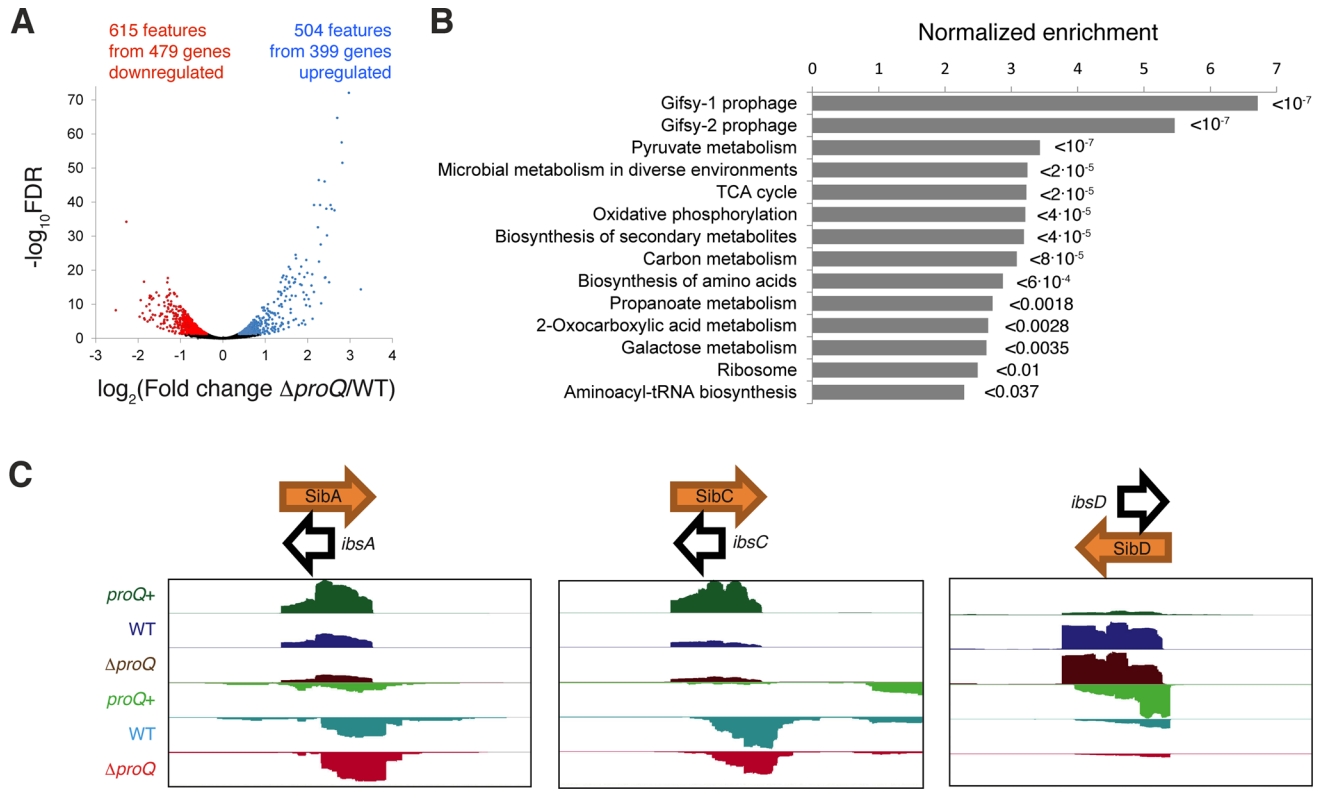

Figure S10. ProQ is a global gene expression regulator in *Salmonella*. (A) Deletion of *proQ* globally affects the gene expression in *Salmonella*. The volcano plot shows the differential expression changes of 8,249 genomic features (coding sequences, UTRs, ncRNAs) plotted against the corresponding FDR values. Features with FDR < 0.05 are highlighted with color. **(B)** KEGG enrichment analysis of the genes differentially affected by *proQ* deletion. Adjusted *P*-values are provided on the right of each category. Only significantly enriched pathways (FDR < 0.05, P_{adj} < 0.05) are shown. **(C)** Examples of *Salmonella* sRNAs (Sib family antitoxins) whose abundance and ability to repress *cis*-encoded mRNA targets (*ibs* mRNAs) depend on ProQ. Read distributions on both strands of three Sib/*ibs* loci in three strains (WT, Δ*proQ* and *proQ*+) are shown scaled to the same height.

SI Tables

Table S1. ProQ-associated sRNAs

sRNA	Genomic coordinates	Features	Enriched in*
art200a	981624<981711	Family of IS200 transposon-associated *cis*-antisense sRNAs	E, T
art200b	1270920<1271007		E, T
art200c (SLnc1010)	1872588>1872675		E, T
art200d (SLnc1011)	2003753>2003840		E, T
art200e (SLnc1020)	2577497>2577584		E, T
art200f	3485887>3485974		E, T
art200g	3657129>3657216		E, T
Ig2335	4162241>4162392		E, T, S
IsrB	1060741>1060834	Prophage *cis*-antisense?	E, S
IsrF	1586723<1587018		E, T
IsrJ	2759644<2759718	Prophage-encoded	S
IsrK	2760478<2760556	Prophage *cis*-antisense	(E), (T), (S)
IstR-1	4019328<4019404	Antitoxins from *tisAB*/IstR type I TA locus	E, T, S
IstR-2	4019328<4019458		E, T, S
RdlD (STnc710, RdlB, StyR-207)	3829661>3829727	Family of antitoxins from *ldr*/Rdl type I TA loci	(T), (S)
RdlE (STnc1060, RdlA, RdlB, StyR-207)	466718<466783		E, T, S
RyfA (tp1, PAIR3)	2672651>2672945		E, T, S
RyfD	2805082<2805222		(E), (T), (S)
RyjB (STnc1120)	1662190<1662282	*Cis*-antisense?	E, T, S
SibA (tp11, RyeC, QUAD1a)	2211623>2211781	Family of antitoxins from *ibs*/Sib type I TA loci	E, T, S
SibC (t27, RygC, QUAD1c)	3243669>3243814		E, T, S
SibD (tp8, C0730, RygD, QUAD1d, StyR-229)	3382993<3383144		E, T, S
SraB (pke20, PsrD)	1231270>1231378	*Trans*-base-paring?	E, S
SraC (RyeA, tpke79, IS091, SLnc0050)	1925543>1925852	*Cis*-antisense?	S
SraF (tpk1, IS160, PsrN, PRE-element)	3412774>3412960	Attenuator	E, S
SraG (PsrO)	3472128>3472312	*Trans*-/*cis*- base-paring	E
SraL (RyjA)	4526162<4526302	*Trans*-/*cis*(?)-base-paring	T, S
RUF_107c.19	223450>223563		T
RUF_107c.23	563424<563507	*Cis*-antisense?	T
RUF_107c.47	3497979<3498072		E, T, S
RUF_107c.58	4311608<4311707	*Cis*-antisense?	T, S
RUF_107c.82	4463078>4463228	*Cis*-antisense?	T
RUF_107c.83	4470487>4470622	*Cis*-antisense?	T
RUF_107c.92	4660039<4660173	*Cis*-antisense?	T
RUF_107c.102	4856253<4856395	*Cis*-antisense?	T
RUF_107c.105	5014>5162	*Cis*-antisense?	T
RUF_107c.112	2368367>2368466	*Cis*-antisense?	E
RUF_111	2285557<2285752		E
SLnc0031	3543523<3543651		(T), (S)
SLnc1015	2459769>2459846	*Cis*-antisense?	E, T, S
sRNA1	257717>257816		E, S
sRNA16	1291395<1291605		T
STnc40	161417>161558	Attenuator?	T, S
STnc310	3413966<3414055	*Cis*-antisense?	E, T
STnc320	3425410>3425649	*Cis*-antisense?	E, T
STnc420	4272916<4272977		E
STnc475	142801>142976		T
STnc520	1290590<1290674		T, S
STnc540	1376238>1376364		E, T, S
STnc610 (*rimP*-leader)	3479058<3479185	Attenuator?	E, S
STnc620	4498083>4498195		E, T, S
STnc670	1170291>1170591		E

STnc750 (sRNA8)	3261186<3261273		S
STnc835	817257>817293		(S)
STnc1030	350913>351102		E
STnc1080 (oop RNA Gifsy-2)	1062745<1062806	Prophage *cis*-antisense?	T, S
STnc1190	4601021>4601437	*Cis*-antisense?	(E), (T), (S)
STnc1200	924756<924838	*Cis*-antisense?	(T), (S)
STnc1275	1992503<1992663		T
STnc1500	138100<138274	*Cis*-antisense?	(S)
STnc1550	2437665>2437808	*Cis*-antisense?	E, T
STnc1565	2488465>2488645		E, T
STnc1640 (StyR-288)	1345903>1345970	*Cis*-antisense?	E, T, S
STnc1650	2133038>2133100	*Cis*-antisense?	E
STnc1690 (STnc1140, RUF_175c.3)	1931467>1931545	*Cis*-antisense?	S
STnc1990	1294843>1294986	*Cis*-antisense?	E
STnc2030	1784648>1784727	*Cis*-antisense?	S
STnc2070	2672472<2672567		E, S
STnc2090	2808307>2808466	*Trans*-base-paring?	E, T, S
STnc2130 (SLnc0038)	4475779>4475869	*Trans*-base-paring?	E, T
STnc2180 (3'ETS(leuZ))	1992864<1992915	sRNA sponge	E
STnc3070	2851167<2851225	*Cis*-antisense?	T
STnc3160	2807823<2807900	*Cis*-antisense?	S
STnc3310	1009199<1009379		E, S
STnc3330	1024493<1024591	*Cis*-antisense?	T
STnc3420	1289667<1289799	*Cis*-antisense?	T
STnc3430	1294946<1295057	*Cis*-antisense?	T
STnc3440	1303294>1303380		T, S
STnc3460	1363845>1363959	*Cis*-antisense?	E, S
STnc3480	1519287>1519550	*Cis*-antisense?	(E)
STnc3510	1506478<1506597		T
STnc3640	1915824>1916082		E
STnc3700	2131885>2131995	*Cis*-antisense?	T
STnc3720	2264259>2264328	*Cis*-antisense?	T
STnc3880	3305410>3305514		E
STnc3970	3507594<3507677	*Cis*-antisense?	T
STnc4130	4796788<4796863	*Cis*-antisense?	E, T, S
STnc4140	4846444<4846540	*Cis*-antisense?	(T), (S)
STnc4190	209868<209971	*Cis*-antisense?	E
STnc4220	1464776<1464883		E
STnc4230	2831959>2832046		E, T, S
STnc4250	4069296>4069505		E, S
StyR-24a	982113>982272	Family of IS200 transposon-associated sRNAs	T
StyR-24d	2003194<2003351		T
StyR-24e	2576935<2577095		T
StyR-24g	3656569<3656727		T
StyR-44e	4219508>4219651	23S rRNA-derived sRNAs	E
StyR-44f	4374472>4374615		E
StyR-44g	4417752>4417894		E
StyR-150	241227>241270	*Cis*-antisense?	T
StyR-199	120107>120156	*Cis*-antisense?	S
StyR-219	3221493>3221564	*Cis*-antisense?	E, T
StyR-243	4365232<4365397	*Cis*-antisense?	E
StyR-248	1502537>1502747	*Cis*-antisense?	T
StyR-291	1883981<1884041	*Cis*-antisense?	T
StyR-305	847583>847697	*Cis*-antisense?	E
StyR-329b (RUF_107c.80)	4426270>4426340		T
StyR-358	751572>751684	*Cis*-antisense?	T

*E - exponential, T - transition, S - stationary phase (based on DESeq2); symbols in parentheses correspond to manually retrieved entries (based on analysis of at least two independent experiments).

Table S2. Bacterial strains used in this study

Strain ID	Genotype	Plasmid	Description
JVS-00007	WT	-	*Salmonella* Typhimurium SL1344 WT
JVS-10315	Δ*proQ::Kan*	-	*Salmonella* Typhimurium SL1344 *proQ* deletion strain created with the use of the lambda-Red system (oligonucleotides JVO-08461/JVO-08462)
JVS-10317	Δ*proQ*	-	JVS-10315 healed with the use of the pCP20 plasmid
JVS-10473	Δ*proQ*	pJV300	JVS-10317 transformed with the control plasmid, used throughout the study as the *proQ* deletion strain
JVS-10474	Δ*proQ*	pZE12-ProQ	JVS-10317 transformed with the complementation plasmid, used throughout the study as the *proQ* complementation strain. The pZE12-luc plasmid contains the *proQ* gene under control of its native promoter (insert created with primers JVO-08523/JVO-08524) cloned into XbaI site in the same orientation as the plasmid-encoded terminator.
JVS-01338	*hfq-3×FLAG*	-	*Salmonella* Typhimurium SL1344 *hfq-3×FLAG* strain
JVS-10314	*proQ-3×FLAG*	-	*Salmonella* Typhimurium SL1344 *proQ-3×FLAG* strain created with the use of the lambda-Red system (oligonucleotides JVO-08728/JVO-08729)
JVS-04317	*csrA-3×FLAG::Kan*	-	*Salmonella* Typhimurium SL1344 *csrA-3×FLAG* strain created with the use of the lambda-Red system (oligonucleotides JVO-03591/JVO-03592)
JVS-10136	*phoP-3×FLAG::Kan*	-	*Salmonella* Typhimurium SL1344 *phoP-3×FLAG* strain created with the use of the lambda-Red system (oligonucleotides JVO-08380/JVO-08381)

Table S3. Oligonucleotides used in this study

Oligo ID	Sequence	Description
JVO-00322	CTACGGCGTTTCACTTCTGAGTTC	Northern blot probe 5S rRNA
JVO-01003	GAATCTCCGAGATGCCG	Northern blot probe 6S RNA
JVO-02181	AAGCAGATTGATAAATGCAACG	Northern blot probe InvR
JVO-03260	CATCTTGCGGTCTGGCA	Northern blot probe art200
JVO-03562	GTGTCTGAAAAACGTACCCTGAT	Northern blot probe MS2 aptamer
JVO-03591	CCAGCGTATCCAGGCTGAAAAATCCCAGCAG TCCAGTTACGACTACAAAGACCATGACGG	Sense oligo for 3×FLAG-tagging CsrA with the use of pSUB11 (2) (to be used with JVO-03592)
JVO-03592	ACCATATCAACAGTGAGGTTGAAAAAAGTCA TGAAGGGACCCATATGAATATCCTCCTTAG	Antisense oligo for 3×FLAG-tagging CsrA with the use of pSUB11 (2) (to be used with JVO-03591)
JVO-03722	ACGTTGACTGGTATAAACCTGGC	Northern blot probe RdlD
JVO-04201	GTTTTTTTTAATACGACTCACTATAGGTCGT ACACCATCAGGGTAC	Universal sense oligo for 5'-MS2 aptamer tagging, carries T7 promoter (to be used with JVO-04203 to create template for MS2 aptamer control on pRR05 (6))
JVO-04202	GTTTTTTTTAATACGACTCACTATAGG	Universal sense oligo for the second PCR step in MS2 aptamer tagging, carries T7 promoter (to be used with an sRNA-specific oligo in 5'-MS2 tagging, or with JVO-04943 in 3'-MS2 tagging)

JVO-04203	GTGACCAGACCCTGATGG	Universal antisense oligo for 3'-MS2 aptamer tagging (to be used with JVO-04201 to create template for MS2 aptamer control on pRR05 (6))
JVO-04943	ACAGACCCTGATGGTGTCT	Antisense oligo to create the MS2 PCR product for 3'-MS2 tagging (to be used with JVO-04943), and a universal antisense oligo for the second PCR in 3'-MS2 tagging (to be used with JVO-04202)
JVO-04944	GTCACCGTACACCATCAGGGTAC	Sense oligo to create the MS2 PCR product for 3'-MS2 tagging (to be used with JVO-04943)
JVO-05974	GGCGATACACTCAATGTAAGGG	Northern blot probe STnc2090
JVO-07694	GTGTCTGGCGAAACGCT	Northern blot probe Msr/STnc400
JVO-08016	CACCATCAGGGTCTGGTCACGAAAAGGCTGAGACCGTTA	Sense oligo for the first PCR in 5'-MS2 tagging STnc1460 (*thi*-box part) (to be used with JVO-08017)
JVO-08017	ATTACTCTTGTTCCCTTCGC	Antisense oligo for 5'-MS2 tagging STnc1460 (*thi*-box part) (to be used with JVO-08016 for the first PCR, and with JVO-04202 for the second PCR)
JVO-08018	GTTTTTTTTAATACGACTCACTATAGGGAAAAGGCTGAGACCGTTA	Sense oligo for the first PCR in 3'-MS2 tagging STnc1460 (*thi*-box part), carries T7 promoter (to be used with JVO-08019)
JVO-08019	GTACCCTGATGGTGTACGGTGACATTACTCTTGTTCCCTTCGC	Antisense oligo for the first PCR in 3'-MS2 tagging STnc1460 (*thi*-box part) (to be used with JVO-08018)
JVO-08044	CACCATCAGGGTCTGGTCACCGCATAATTTAAGACCGC	Sense oligo for the first PCR in 5'-MS2 tagging STnc1640 (to be used with JVO-08045)
JVO-08045	ATAAAGAAAACCGCCGAT	Antisense oligo for 5'-MS2 tagging STnc1640 (to be used with JVO-08044 for the first PCR, and with JVO-04202 for the second PCR)
JVO-08046	GTTTTTTTTAATACGACTCACTATAGGCGCATAATTTAAGACCGC	Sense oligo for the first PCR in 3'-MS2 tagging STnc1640, carries T7 promoter (to be used with JVO-08047)
JVO-08047	GTACCCTGATGGTGTACGGTGACATAAAGAAAACCGCCGAT	Antisense oligo for the first PCR in 3'-MS2 tagging STnc1640 (to be used with JVO-08046)
JVO-08075	CACCATCAGGGTCTGGTCACACTCTTTAGCGTTAGGCTTTG	Sense oligo for the first PCR in 5'-MS2 tagging STnc400 (to be used with JVO-08076)
JVO-08076	AAAAGTACTCAATAAGTTAGTGTCTGG	Antisense oligo for 5'-MS2 tagging Pre-Msr/STnc400 (to be used with JVO-08151 for the first PCR, and with JVO-04202 for the second PCR)
JVO-08077	GTTTTTTTTAATACGACTCACTATAGGACTCTTTAGCGTTAGGCTTTG	Sense oligo for the first PCR in 3'-MS2 tagging Pre-Msr/STnc400, carries T7 promoter (to be used with JVO-08078)
JVO-08078	GTACCCTGATGGTGTACGGTGACAAAAGTACTCAATAAGTTAGTGTCTGG	Antisense oligo for the first PCR in 3'-MS2 tagging Pre-Msr/STnc400 (to be used with JVO-08152)
JVO-08149	CACCATCAGGGTCTGGTCACCCCCCTCTTCGGAGG	Sense oligo for the first PCR in 5'-MS2 tagging STnc1460 (to be used with JVO-08150)
JVO-08150	GTTTTTTTTAATACGACTCACTATAGGCCCCCTCTTCGGAGG	Antisense oligo for 5'-MS2 tagging STnc1460 (to be used with JVO-08149 for the first PCR, and with JVO-04202 for the second PCR)
JVO-08164	TTCATCGTTATTATTATCCCG	Northern blot probe ChiX
JVO-08376	CACCATCAGGGTCTGGTCACAATTGATCAACAAGCTGGAAC	Sense oligo for the first PCR in 5'-MS2 tagging STnc2090 (to be used with JVO-08377)
JVO-08377	CGCGCCCGAAGGCGCGTTGG	Antisense oligo for 5'-MS2 tagging STnc2090 (to be used with JVO-08376 for the first PCR, and with JVO-04202 for the second PCR)
JVO-08378	GTTTTTTTTAATACGACTCACTATAGGAATTGATCAACAAGCTGGAAC	Sense oligo for the first PCR in 3'-MS2 tagging STnc2090, carries T7 promoter (to be used with JVO-08379)
JVO-08379	GTACCCTGATGGTGTACGGTGACCGCGCCCGAAGGCGCGTTGG	Antisense oligo for the first PCR in 3'-MS2 tagging STnc2090 (to be used with JVO-08378)
JVO-08380	TACCACCGTACGCGGACAAGGATATCTTTTTGAATTGCGCGACTACAAAGACCATGACGG	Sense oligo for 3×FLAG-tagging PhoP with the use of pSUB11 (2) (to be used with JVO-08381)

JVO-08381	CGCAGCGACAGCGGCAGAAAATGGCGAGCAA ATTTATTCACATATGAATATCCTCCTTAG	Antisense oligo for 3×FLAG-tagging PhoP with the use of pSUB11 (2) (to be used with JVO-08380)
JVO-08405	TTTGCGCTGGCGACCAGATG	Northern blot probe *raiA* mRNA
JVO-08461	CAACGGATAACGTAGCAATTACTGATGGCGT CATTATAATGTGTAGGCTGGAGCTGCTTC	Sense oligo for deletion of *proQ* in *Salmonella* with the use of pKD4 (1) (to be used with JVO-08462)
JVO-08462	CGGTTTATCAGCGCGAGGTTTACGTTCAGCG CCTTCTTTACATATGAATATCCTCCTTAG	Antisense oligo for deletion of *proQ* in *Salmonella* with the use of pKD4 (1) (to be used with JVO-08461)
JVO-08493	CATACTGGTGATACTCTTAGTG	Northern blot probe SibA
JVO-08495	ATGCAACGGCCTCTGCTT	Northern blot probe *cspD* mRNA
JVO-08497	TGTTAATCATCGCTTGCCCA	Northern blot probe SibC
JVO-08498	GAGGTTCCGGTTTGTGTTGAT	Northern blot probe SraL
JVO-08515	GGTGGTTGCTCTTCCAACATGGAAAATCAAC CTAAGTTGAATAGC	Sense oligo to amplify *Salmonella proQ* ORF for cloning into pTYB11, SapI site (to be used with JVO-08516)
JVO-08516	GGTGGTCTGCAGTCATCAGAACACCAGGTGT TCTGCGCG	Antisense oligo to amplify *Salmonella proQ* ORF for cloning into pTYB11, PstI site (to be used with JVO-08515)
JVO-08523	AGGCGTCTCTAGATACCGAAGAAGATGAACA CGGCC	Sense oligo to amplify *Salmonella proQ* ORF for cloning into pZE12-luc, XbaI site (to be used with JVO-08524)
JVO-08524	AGGCGTCTCTAGAAAAAAAAGTGTTCATGCC AGGCC	Antisense oligo to amplify *Salmonella proQ* ORF for cloning into pZE12-luc, XbaI site (to be used with JVO-08523)
JVO-08540	CCTCCGACCCCTTCG	Northern blot probe $tRNA^{Pro}_{CGG}$
JVO-08543	GTTTTTTTTAATACGACTCACTATAGGTTGA CATTATTCTTGATGTGGC	Sense oligo to create template for SibA *in vitro* transcription, carries T7 promoter (to be used with JVO-08544)
JVO-08544	AAAATAAGGAAAAGGGTTATGATGAAGG	Antisense oligo to create template for SibA *in vitro* transcription, (to be used with JVO-08543)
JVO-08551	CCCAAAACGTGAGTAAGTATCTA	Northern blot probe STnc475
JVO-08720	CACCATCAGGGTCTGGTCACAGACCGAATAC GATTCC	Sense oligo for the first PCR in 5'-MS2 tagging SraC (to be used with JVO-08721)
JVO-08721	CGCAAACTGGAAAACCTGG	Antisense oligo for 5'-MS2 tagging SraC (to be used with JVO-08720 for the first PCR, and with JVO-04202 for the second PCR)
JVO-08722	GTTTTTTTTAATACGACTCACTATAGGAGAC CGAATACGATTCC	Sense oligo for the first PCR in 3'-MS2 tagging SraC, carries T7 promoter (to be used with JVO-08723)
JVO-08723	GTACCCTGATGGTGTACGGTGACCGCAAACT GGAAAACCTGG	Antisense oligo for the first PCR in 3'-MS2 tagging SraC (to be used with JVO-08722)
JVO-08728	GGGTATGTCTTTGATTGTACGCGCAGAACAC CTGGTGTTCGACTACAAAGACCATGACGG	Sense oligo for 3×FLAG-tagging ProQ in *Salmonella* with the use of pSUB11 (2) (to be used with JVO-08729)
JVO-08729	AAGCCTAAAAAAAGTGTTCATGCCAGGCCTG GCCTCCGTTCATATGAATATCCTCCTTAG	Antisense oligo for 3×FLAG-tagging ProQ in *Salmonella* with the use of pSUB11 (2) (to be used with JVO-08728)
JVO-10325	TGGTGGAGCTGGCGGGAGTT	Northern blot probe tmRNA
JVO-10346	GTTTTTTTTAATACGACTCACTATAGGATTG ATCAACAAGCTGGAACG	Sense oligo to create template for STnc2090 *in vitro* transcription, carries T7 promoter (to be used with JVO-10347)
JVO-10347	AAAAAACGCGCCCGAAG	Antisense oligo to create template for STnc2090 *in vitro* transcription, (to be used with JVO-10346)
JVO-10931	GCTTTGGGAACTAGCGAATC	Northern blot probe SLnc1015
JVO-11060	GCCAATAATTCGCACACATTGC	Northern blot probe SraB
JVO-11395	CACCATCAGGGTCTGGTCACAGTCGAGTAAC GTCGGTG	Sense oligo for the first PCR in 5'-MS2 tagging STnc475 (to be used with JVO-11396)
JVO-11396	AGAGAAGGTGGCCCTCTC	Antisense oligo for 5'-MS2 tagging STnc475 (to be used with JVO-11395 for the first PCR, and with JVO-04202 for the second PCR)

JVO-11397	GTTTTTTTTAATACGACTCACTATAGGAGTC GAGTAACGTCGGTG	Sense oligo for the first PCR in 3'-MS2 tagging STnc475, carries T7 promoter (to be used with JVO-11398)
JVO-11398	GTACCCTGATGGTGTACGGTGACAGAGAAGG TGGCCCTCTC	Antisense oligo for the first PCR in 3'-MS2 tagging STnc475 (to be used with JVO-11397)
JVO-11399	CACCATCAGGGTCTGGTCACCTTTCCGCGCC CTGGTTTTAC	Sense oligo for the first PCR in 5'-MS2 tagging STnc1565 (to be used with JVO-11400)
JVO-11400	AAAGCGCGCCCTGTCG	Antisense oligo for 5'-MS2 tagging STnc1565 (to be used with JVO-11399 for the first PCR, and with JVO-04202 for the second PCR)
JVO-11401	GTTTTTTTTAATACGACTCACTATAGGCTTT CCGCGCCCTGGTTTTAC	Sense oligo for the first PCR in 3'-MS2 tagging STnc1565, carries T7 promoter (to be used with JVO-11402)
JVO-11402	GTACCCTGATGGTGTACGGTGACAAAGCGCG CCCTGTCG	Antisense oligo for the first PCR in 3'-MS2 tagging STnc1565 (to be used with JVO-11401)
JVO-11518	CTCCTGACCCTCATCCTGAGTCG	Northern blot probe CsrC
JVO-11694	CACCATCAGGGTCTGGTCACGGGGCTATAGC TCAGCTGGG	Sense oligo for the first PCR in 5'-MS2 tagging $tRNA^{Ala}_{TGC}$ (to be used with JVO-11695)
JVO-11695	TGGAGCTATGCGGGATCG	Antisense oligo for 5'-MS2 tagging $tRNA^{Ala}_{TGC}$ (to be used with JVO-11694 for the first PCR, and with JVO-04202 for the second PCR)
JVO-12159	CACCATCAGGGTCTGGTCACTTTCTCTGAGA TGTTTGCAAGCGGGCCAG	Sense oligo for the first PCR in 5'-MS2 tagging 6S RNA (to be used with JVO-12160)
JVO-12160	GAATCTCCGAGATGCCGCCGC	Antisense oligo for 5'-MS2 tagging 6S RNA (to be used with JVO-12159 for the first PCR, and with JVO-04202 for the second PCR)
JVO-12161	GTTTTTTTTAATACGACTCACTATAGGTTTC TCTGAGATGTTTGCAAGCGGGCCAG	Sense oligo for the first PCR in 3'-MS2 tagging 6S RNA, carries T7 promoter (to be used with JVO-12162)
JVO-12162	GTACCCTGATGGTGTACGGTGACGAATCTCC GAGATGCCGCCGC	Antisense oligo for the first PCR in 3'-MS2 tagging 6S RNA (to be used with JVO-12161)
JVO-12249	CACCATCAGGGTCTGGTCACGAAGGGTGAGG GAGGCG	Sense oligo for the first PCR in 5'-MS2 tagging SibC (to be used with JVO-12250)
JVO-12250	GGGAAAGCCCCTACCGAGGC	Antisense oligo for 5'-MS2 tagging SibC (to be used with JVO-12249 for the first PCR, and with JVO-04202 for the second PCR)
JVO-12255	CACCATCAGGGTCTGGTCACGCCTTAACAGC ACCCCGATATATC	Sense oligo for the first PCR in 5'-MS2 tagging IsrB (to be used with JVO-12256)
JVO-12256	GAAAACGCCCACCGAAGCGGGC	Antisense oligo for 5'-MS2 tagging IsrB (use with JVO-12255 for the first PCR, and with JVO-04202 for the second PCR)
JVO-12261	CACCATCAGGGTCTGGTCACTTTTAAGCACC GGCGTTTGC	Sense oligo for the first PCR in 5'-MS2 tagging as*yhbQ* (to be used with JVO-12262)
JVO-12262	TTAACGCTGGCGTTTGCGGC	Antisense oligo for 5'-MS2 tagging as*yhbQ* (to be used with JVO-12261 for the first PCR, and with JVO-04202 for the second PCR)
JVO-12267	CACCATCAGGGTCTGGTCACCTAATGCCGGA TGGCGGCG	Sense oligo for the first PCR in 5'-MS2 tagging STnc1560 (to be used with JVO-12268)
JVO-12268	AGAATGCCGGATGGCGATGC	Antisense oligo for 5'-MS2 tagging STnc1560 (to be used with JVO-12267 for the first PCR, and with JVO-04202 for the second PCR)
JVO-12270	CACCATCAGGGTCTGGTCACCTTAATTGCCA ATCAATGTCTGATGGC	Sense oligo for the first PCR in 5'-MS2 tagging RUF 107c.58 (to be used with JVO-12271)
JVO-12271	ATAAATGCCGGATGGCGGC	Antisense oligo for 5'-MS2 tagging RUF 107c.58 (to be used with JVO-12270 for the first PCR, and with JVO-04202 for the second PCR)

SI Datasets

Dataset S1. Grad-seq profiles of *Salmonella* Typhimurium SL1344 transcripts in 10-40% glycerol gradient, based on the fraction-wise RNA-seq. Only the profiles with ≥30 reads in at least one fraction are shown. All profiles are standardized to the range from 0 to 1.

Dataset S2. Sedimentation profiles of *Salmonella* Typhimurium SL1344 proteins in 10-40% glycerol gradient, based on the fraction-wise LC-MS/MS. Only profiles with ≥5 spectral counts in the peaking fraction are retained. All profiles are standardized to the range from 0 to 1.

Dataset S3. Enrichments of *Salmonella* Typhimurium SL1344 transcripts in ProQ coIP experiments. Transcripts significantly enriched over two medians (according to DESeq2) in each growth phase are highlighted.

Dataset S4. Differential gene expression analysis of the *Salmonella* Typhimurium SL1344 Δ*proQ* strain vs the parental WT.

SI References

1. Datsenko KA & Wanner BL (2000) One-step inactivation of chromosomal genes in Escherichia coli K-12 using PCR products. *Proc Natl Acad Sci USA* 97(12):6640-6645.
2. Uzzau S, Figueroa-Bossi N, Rubino S, & Bossi L (2001) Epitope tagging of chromosomal genes in Salmonella. *Proc Natl Acad Sci USA* 98(26):15264-15269.
3. Kunte HJ, Crane RA, Culham DE, Richmond D, & Wood JM (1999) Protein ProQ influences osmotic activation of compatible solute transporter ProP in Escherichia coli K-12. *J Bacteriol* 181(5):1537-1543.
4. Förstner KU, Vogel J, & Sharma CM (2014) READemption-a tool for the computational analysis of deep-sequencing-based transcriptome data. *Bioinformatics*.
5. Erickson HP (2009) Size and shape of protein molecules at the nanometer level determined by sedimentation, gel filtration, and electron microscopy. *Biol Proced Online* 11:32-51.
6. Said N, *et al.* (2009) In vivo expression and purification of aptamer-tagged small RNA regulators. *Nucleic Acids Res* 37(20):e133.

7. Ching T, Huang S, & Garmire LX (2014) Power analysis and sample size estimation for RNA-Seq differential expression. *RNA* 20(11):1684-1696.
8. Love MI, Huber W, & Anders S (2014) Moderated estimation of fold change and dispersion for RNA-seq data with DESeq2. *Genome Biol* 15(12):550.
9. Bonn F *et al.* (2014) Picking vanished proteins from the void: how to collect and ship/share extremely dilute proteins in a reproducible and highly efficient manner. *Anal Chem* 86(15):7421-7427.
10. Risso D, Ngai J, Speed TP, & Dudoit S (2014) Normalization of RNA-seq data using factor analysis of control genes or samples. *Nat Biotechnol* 32(9):896-902.
11. Wessa P (2014) Free Statistics Software, Office for Research Development and Education, version 1.1.23-r7. http://www.wessa.net/.
12. Kirkman TW (1996) Statistics to use. http://www.physics.csbsju.edu/stats/.
13. Papadopoulos JS & Agarwala R (2007) COBALT: constraint-based alignment tool for multiple protein sequences. *Bioinformatics* 23(9):1073-1079.
14. Chaulk S*, et al.* (2010) *N. meningitidis* 1681 is a member of the FinO family of RNA chaperones. *RNA Biol* 7(6):812-819.
15. Creevey CJ & McInerney JO (2005) Clann: investigating phylogenetic information through supertree analyses. *Bioinformatics* 21(3):390-392.
16. Letunic I & Bork P (2011) Interactive Tree Of Life v2: online annotation and display of phylogenetic trees made easy. *Nucleic Acids Res* 39(Web Server issue):W475-478.
17. Hofacker IL*, et al.* (1994) Fast Folding and Comparison of Rna Secondary Structures. *Monatsh Chem* 125(2):167-188.
18. Ghetu AF, Gubbins MJ, Frost LS, & Glover JN (2000) Crystal structure of the bacterial conjugation repressor finO. *Nat Struct Biol* 7(7):565-569.